

Manuscript Number: LITHOS6950R1

Title: Evidence of Permian magmatism in the Alpi Apuane Metamorphic Complex (Northern Apennines, Italy): new hints for the geological evolution of the basement of the Adria plate

Article Type: Regular Article

Keywords: Metarhyolite; Permian magmatism; U-Pb LA-ICP-MS zircon chronology; Paleozoic basement; Alpi Apuane

Corresponding Author: Dr. Cristian Biagioni,

Corresponding Author's Institution: Università di Pisa

First Author: Simone Vezzoni

Order of Authors: Simone Vezzoni; Cristian Biagioni; Massimo D'Orazio; Diego Pieruccioni; Yuri Galanti; Maurizio Petrelli; Giancarlo Molli

**Abstract:** The occurrence of metavolcanic rocks within the Paleozoic basement of the Alpi Apuane Metamorphic Complex has been known since long time. Among them, some massive porphyritic tourmaline-bearing rocks cropping out in the southern sector of the Alpi Apuane present some distinctive and peculiar features, differing from the better known middle Ordovician metarhyolites of the "Porfiroidi e scisti porfirici" Fm. The porphyritic tourmaline-bearing rocks belong to the recently proposed Fornovolasco Metarhyolite Fm. They are granular to porphyritic, with phenocrysts of quartz (sometimes with magmatic embayment), feldspar, and mica (both biotite and muscovite), in a groundmass formed by quartz, white mica, and feldspar. Tourmaline (schorl-dravite in composition) is an abundant accessory mineral, in some cases forming cm-sized spots. The studied rocks plot into the rhyolite field of the Total Alkali vs Silica classification diagram. They show a peraluminous nature, having an Alumina Saturation Index ranging from 1.3 and 3.2. Their trace-element signature is that typical of highly evolved orogenic magmas. Laser ablation-ICP-MS U-Pb datings on zircon suggest a Permian crystallization age (weighted average ages of the four samples ranging from 292 and 271 Ma), thus relating these rocks to a post-Variscan magmatism. This new dating represents the very first evidence of a Permian magmatism in the pre-Triassic basement of the Northern Apennines. The potential relationships between Permian felsic magmatism and the ore genesis in the Alpi Apuane Metamorphic Complex are also discussed.

## Revision 1

# Evidence of Permian magmatism in the Alpi Apuane Metamorphic Complex (Northern Apennines, Italy): new hints for the geological evolution of the basement of the Adria plate

Simone Vezzoni<sup>1</sup>, Cristian Biagioni<sup>1\*</sup>, Massimo D'Orazio<sup>1</sup>, Diego Pieruccioni<sup>1</sup>, Yuri Galanti<sup>1</sup>,  
Maurizio Petrelli<sup>2,3</sup>, and Giancarlo Molli<sup>1</sup>

<sup>1</sup> *Dipartimento di Scienze della Terra, Università di Pisa, Via S. Maria 53, I-56126, Pisa, Italy*

<sup>2</sup> *Dipartimento di Fisica e Geologia, Università di Perugia, Piazza dell'Università, I-06123  
Perugia, Italy*

<sup>3</sup> *Istituto Nazionale di Fisica Nucleare, Sezione di Perugia, Via Alessandro Pascoli 23c, I-06123  
Perugia, Italy*

\*Corresponding author: [cristian.biagioni@unipi.it](mailto:cristian.biagioni@unipi.it)

## 1. Introduction

The Paleozoic basement of the Northern Apennines (central-northern Italy) has been described from few small outcrops, with the only exception being represented by the Alpi Apuane where large outcrops (ca. 60 km<sup>2</sup>) of pre-Triassic formations are widely exposed. During the Alpine tectonic evolution, these formations were part of the basement of the Adria plate which, according to different authors (e.g., Stampfli and Borel, 2002; Stampfli et al., 2002; von Raumer et al., 2013), was located, in the Paleozoic paleotectonic frame, along the northern margin of Gondwana, therefore recording the tectono-sedimentary and magmatic processes associated with its

geodynamic evolution (e.g., Sirevaag et al., 2017). Indeed, during the late Neoproterozoic-middle Paleozoic, the northern margin of Gondwana was modified first by crustal accretion and then by repeated rifting and associated intense magmatism (e.g., Romeo et al., 2006; von Raumer et al., 2013). In the late Paleozoic, many Gondwana-derived continental fragments, among which part of the future Adria plate, were incorporated into the Variscan orogeny, deformed at different *P-T* conditions, and affected by extensive magmatism occurred during both the collisional and post-collisional phases (e.g., Kroner and Romer, 2013). Such events have been differently recorded in the Paleozoic basement units of several circum-Mediterranean chains (von Raumer et al., 2013).

Several difficulties in the interpretation of this record in the Northern Apennine basement have been encountered by previous authors, mainly owing to the small and scattered outcrops, the rarity of fossiliferous layers in metasedimentary units, and the Alpine metamorphic overprint, usually obliterating or masking the older structures. Moreover, very few geochronological data are available to date. Indeed, the present knowledge of the basement stratigraphy derives mainly from geological, petrographical, and geochemical data, coupled with a correlation with the better known and well-dated Paleozoic sequences of central Sardinia, allowing some tentative stratigraphic reconstructions (e.g., Pandeli et al., 1994 and references therein). Only recently, Musumeci et al. (2011), Sirevaag et al. (2017), and Paoli et al. (2017) reported U-Pb dating on detrital as well as magmatic zircon from rocks belonging to the basement of the Northern Apennines, giving a significant contribution to its stratigraphy.

The stratigraphic succession of the Alpi Apuane suffers the same lack of geochronological data common to the other outcrops of Northern Apennines. In addition to the biostratigraphical dating of Vai (1972) and Bagnoli and Tongiorgi (1980), the only available geochronological data were given by Paoli et al. (2017). These authors suggested early Cambrian depositional ages for both the “*Filladi inferiori*” (Lower Phyllites) and “*Filladi superiori*” (Upper Phyllites) Fms, and a crystallization age of  $457 \pm 3$  Ma for the “*Porfiroidi e scisti porfirici*” (Porphyroids and Porphyritic Schists) Fm. The Alpi Apuane represent not only a privileged area for the study of the older

formations recording the evolution of the northern Gondwana margin up to their incorporation into the Variscan orogenic belt, but also for the investigation of several polymetallic ore deposits, mostly related to hydrothermal circulation within the Paleozoic basement.

Within the frame of an ongoing study of the mineralogy, geochemistry, and structural setting of such ore deposits from the southern Alpi Apuane, a close spatial relationship between the pyrite  $\pm$  baryte  $\pm$  iron oxide  $\pm$  (Pb-Zn-Ag) ore deposits (D'Orazio et al., 2017) and felsic, tourmaline-rich, meta-igneous rock bodies belonging to the Paleozoic basement was observed. Such bodies may achieve a length of more than 1 km and an apparent thickness larger than 100 m (Pieruccioni et al., 2018). This peculiar association, as well as the massive nature of these rock bodies, completely different from the surrounding schists, promoted a field survey of these rocks, known since the end of the 19<sup>th</sup> Century (e.g., Lotti, 1882), integrated by petrographic, geochemical, and geochronological data. In this paper, the results of this study are reported, emphasizing both the geodynamic significance of such rocks in the framework of the Adria plate basement evolution and their implications for the hydrothermal processes affecting the Paleozoic sequences of the Alpi Apuane.

## **2. Geological framework of Alpi Apuane**

### *2.1. Geological background*

The Northern Apennines are an orogenic belt formed during the Oligocene-Miocene collision between the Corsica-Sardinia microplate and the Adria plate. As a consequence of this collision, stacked slices of the former Adria plate continental margin (Tuscan and external foreland tectonic units) lie below the ocean-derived, ophiolite-bearing, Ligurian units. The Tuscan units locally preserve the Paleozoic basement overlain by Mesozoic and Cenozoic cover sequences (Molli, 2008 and references therein).

78 In the Alpi Apuane area, a large tectonic window exposes the lowermost units of the inner side  
79 of the Northern Apennines, represented by the Apuane and Massa units (Fig. 1). These units were  
80 affected by regional metamorphism under moderate pressure greenschist facies conditions during  
81 late Oligocene-early Miocene (e.g., Di Pisa et al., 1985; Franceschelli et al., 1986; Jolivet et al.,  
82 1998; Franceschelli et al., 2004; Fellin et al., 2007, and references therein). The present structural  
83 setting is the result of two main tectono-metamorphic events (D1 and D2, according to Carmignani  
84 and Kligfield, 1990), related to the deformation of the Adria plate continental margin during the  
85 continent-continent collision and the syn- to post-contractional exhumation (e.g., Molli, 2008).

86 The studied area (Fig. 2) is located in the southern part of the Alpi Apuane and extends along a  
87 narrow SW-NE belt, ca. 10 km in length, running from the village of Valdicastello Carducci, near  
88 the small city of Pietrasanta, to the hamlet of Fornovolasco. Its position completely overlaps with  
89 the discontinuous mineralized belt known for the occurrence of pyrite  $\pm$  baryte  $\pm$  iron oxide  $\pm$  (Pb-  
90 Zn-Ag) ore deposits (D'Orazio et al., 2017). In this area, the metamorphic rocks belonging to the  
91 Apuane Unit crop out below the Tuscan Nappe in two tectonic windows, i.e., the Sant'Anna and  
92 Fornovolasco tectonic windows, in the SW and NE corners of this belt, respectively, and in the  
93 Stazzemese area, in the central part of the studied area. The Apuane Unit is here characterized by  
94 km-scale recumbent D2 isoclinal folds and tectonic slices, with rocks of the Paleozoic basement  
95 locally overlying the younger Meso-Cenozoic metasedimentary sequences. The Paleozoic basement  
96 cropping out in the studied area is composed of metasiliciclastic rocks with local intercalations of  
97 lenses of porphyritic tourmaline-rich rocks and shows some peculiar features with respect to the  
98 other outcrops of basement rocks occurring in the Alpi Apuane. Indeed, it is characterized by a  
99 widespread tourmalinization and by the occurrence of several small ore deposits embedded in the  
100 basement or close to the contact with the Triassic metadolostone ("*Grezzoni*" Fm). As a  
101 consequence, some authors proposed different interpretations of this lithostratigraphic succession,  
102 in some cases using specific formational names to identify it (e.g., "Fornovolasco Schists" – Pandeli  
103 et al., 2004). Other authors proposed a correlation between this peculiar succession and the

104 remaining part of the pre-Triassic basement of the Apuane Unit, identifying the metasedimentary  
105 rocks with the “*Filladi inferiori*” Fm and the interlayered lenses of porphyritic tourmaline-rich  
106 rocks with the “*Porfiroidi e scisti porfirici*” Fm (Carmignani et al., 1976; Pandeli et al., 2004).

107

## 108 2.2. The metavolcanic rocks

109

110 The occurrence of metavolcanic rocks within the Paleozoic basement of Alpi Apuane has been  
111 known since the end of the 19<sup>th</sup> Century, even if the first comprehensive petrographical study was  
112 performed by Bonatti (1938).

113 The “*Porfiroidi e scisti porfirici*” Fm (Barberi and Giglia, 1965) represents the main felsic  
114 metavolcanic rocks (“*Porfiroidi*”) and their subaerial reworking products (“*Scisti Porfirici*”)  
115 occurring in the basement of Alpi Apuane. These rocks are characterized by a primary porphyritic  
116 texture and well-developed foliations related to both the Variscan and Alpine tectono-metamorphic  
117 events (Conti et al., 1991). They show a distinct augen texture, with large magmatic phenocrysts of  
118 quartz (usually with magmatic embayment) and K-feldspar, in a fine-grained matrix formed by  
119 muscovite, quartz, and chlorite (Barberi and Giglia, 1965). Chemical data indicate a rhyolitic/dacitic  
120 composition for the volcanic protolith (e.g., Puxeddu et al., 1984).

121 The age of these rocks has long been debated. Indeed, different authors proposed ages ranging  
122 from Permian (e.g., Barberi and Giglia, 1965) to middle Ordovician (e.g., Gattiglio et al., 1989).  
123 This latter age was proposed correlating the “*Porfiroidi e scisti porfirici*” Fm with similar  
124 metavolcanic products occurring in Sardinia. Recently, Paoli et al. (2017) confirmed such an age  
125 attribution through U-Pb zircon dating, indicating a crystallization age of  $457 \pm 3$  Ma, similar to that  
126 reported for the Ortano Porphyroids (Elba Island) by Musumeci et al. (2011) and Sirevaag et al.  
127 (2017) and for the calc-alkaline effusive magmatic rocks of the Variscan chain occurring in the  
128 Paleozoic basement of Sardinia, dated at  $465 \pm 1$  Ma (Oggiano et al., 2010) and  $448 \pm 5$  Ma  
129 (Cruciani et al., 2013).

130 Locally, the “*Porfiroidi e scisti porfirici*”, as well as the “*Filladi inferiori*” Fms, host small  
131 bodies of greenish and grey-greenish metabasites, tentatively assigned to a late to post-Ordovician  
132 magmatism (e.g., Conti et al., 1988, 1993).

133 The lenticular bodies of porphyritic tourmaline-rich rocks occurring within the Paleozoic  
134 phyllites in the southern Alpi Apuane have attracted the attention of several geologists during the  
135 second half of the 19<sup>th</sup> Century and the first decades of the 20<sup>th</sup> Century, mainly owing to their  
136 massive nature, contrasting with the surrounding strongly foliated schists. The first petrographic  
137 description was given by Bonatti (1933), who described the small outcrop of Le Casette, near the  
138 hamlet of Fornovolasco (Fig. 2). This lithology is mainly composed of quartz (sometimes showing  
139 magmatic embayment), tourmaline, feldspar, and muscovite. Accessory minerals are represented by  
140 apatite and rutile. According to Bonatti (1933), this rock could be interpreted as a meta-tufite. Since  
141 then, the interpretation of the stratigraphic significance of these tourmaline-rich rocks has been  
142 debated. For instance, Conti et al. (2012) described such rocks as a potential Tertiary aplite,  
143 whereas Pandeli et al. (2004) related them to the middle Ordovician “*Porfiroidi*”. Finally, following  
144 the new data obtained during the present study, Pieruccioni et al. (2018) proposed a distinction  
145 between these rock bodies and the “*Porfiroidi*”, defining the “Fornovolasco Metarhyolite” Fm.

146

### 147 **3. Samples and methods**

148

149 The samples studied in this work represent all the major known occurrences of the rocks  
150 belonging to the Fornovolasco Metarhyolite Fm in the Alpi Apuane (Fig. 2; Table 1). For the sake  
151 of comparison, three samples of “*Porfiroidi*” (Fig. 1; Table 1), showing the same petrographic  
152 features previously described by Barberi and Giglia (1965), were geochemically characterized.

153 The petrographic features of the rock samples were investigated by optical microscopy  
154 integrated by Scanning Electron Microscopy (SEM) observations. A SEM Philips XL 30 operating  
155 at 20 kV accelerating voltage and 5 µm beam diameter coupled with an energy-dispersive X-ray

156 fluorescence spectrometer EDAX PV 9900 at the Pisa University's Dipartimento di Scienze della  
157 Terra was used. Electron-microprobe analyses were performed to fully characterize their  
158 mineralogy. Chemical data have been collected using an automated JEOL 8200 Super Probe at the  
159 Milano University's Dipartimento di Scienze della Terra "Ardito Desio". Operating conditions were  
160 15 kV accelerating voltage, beam current of 5 nA, and 3  $\mu\text{m}$  beam size, using wavelength dispersive  
161 spectrometry (WDS). A  $\phi(\rho Z)$  routine was used for matrix correction (Pouchou and Pichoir, 1991).  
162 Standards (element, emission line) were: omphacite ( $\text{NaK}\alpha$ ), K-feldspar ( $\text{KK}\alpha$ ), rhodonite ( $\text{MnK}\alpha$ ),  
163 olivine ( $\text{MgK}\alpha$ ), grossular ( $\text{AlK}\alpha$ ,  $\text{SiK}\alpha$ ,  $\text{CaK}\alpha$ ), fayalite ( $\text{FeK}\alpha$ ), apatite ( $\text{PK}\alpha$ ), ilmenite ( $\text{TiK}\alpha$ ),  
164 nickeline ( $\text{NiK}\alpha$ ), metal Cr ( $\text{CrK}\alpha$ ), hornblende ( $\text{FK}\alpha$ ), celestine ( $\text{SrL}\alpha$ ), metal V ( $\text{VK}\alpha$ ), and  
165 sanbornite ( $\text{BaL}\alpha$ ). Counting times were 30 s for peak and 10 s for left and right backgrounds.

166 Chemical analyses of whole rocks were performed at ACTLABS (Ancaster, Ontario, Canada).  
167 Major and trace elements were determined by ICP-OES and ICP-MS, respectively, following  
168 lithium metaborate/tetraborate fusion and dissolution with diluted  $\text{HNO}_3$ .

169 Geochronological data were obtained by zircon U-Pb analyses on four samples (FVb13, FVc1,  
170 POL1, and SAS1). After crushing and sieving, zircon crystals were concentrated from the 90-250  
171  $\mu\text{m}$  grain size interval using standard separation techniques. About 100 zircon crystals for each  
172 sample were embedded in epoxy resin, ground to expose approximately mid-section of crystals, and  
173 finally polished with 0.25  $\mu\text{m}$  alumina paste. Crystals for geochronological analyses were selected  
174 using SEM-cathodoluminescence (SEM-CL) taking into account the occurrence of inclusions, cores  
175 and/or rims and compositional zoning. Laser Ablation-Inductively Coupled Plasma-Mass  
176 Spectrometry (LA-ICP-MS) U-Pb analyses were performed at the Perugia University's  
177 Dipartimento di Fisica e Geologia using an iCAPQ Thermo Fisher Scientific, quadrupole-based,  
178 ICP-MS coupled to a G2 Teledyne Photon Machine ArF (193 nm) LA system. Uranium-Pb zircon  
179 analyses were calibrated with the international reference material zircon 91500 using a spot size of  
180 25  $\mu\text{m}$  and the Plešovice zircon had been used as quality control (Sláma et al., 2008). Data  
181 reduction was performed by the VizualAge protocol (Petrus and Kamber, 2012). In particular, raw



182 signal counts and their ratios were carefully monitored in order to exclude from age calculations  
183 portions that may be contaminated by inclusions and/or spurious peaks. In addition, complex  
184 signals that may represent multiple ages had been carefully inspected to avoid misleading  
185 interpretations of the profiles. Net background-corrected count rates for each isotope were used for  
186 calculation (for further details, Petrelli et al., 2016). The analytical data were treated using the  
187 Isoplot Excel toolkit (Ludwig, 2003). The  $^{206}\text{Pb}/^{238}\text{U}$  ages were used for probability plots.

188

## 189 **4. Results**

190

### 191 *4.1. Field study*

192

193 The rocks belonging to the Fornovolasco Metarhyolite Fm (Figg. 3, 4) are granular to  
194 porphyritic and white to dark-grey in color. Locally, tourmaline spots, up to some cm in size and  
195 with a leucocratic rim halo, occur (Fig. 3a). This latter feature is particularly developed in the large  
196 outcrop of the Boscaccio locality, east of Fornovolasco, whereas it is rarer in the other outcrops.  
197 The most striking feature is the massive nature of these rocks (Fig. 3). Only locally, they show a  
198 spaced foliation, more evident towards the contact with the country schists, belonging to the  
199 “*Filladi inferiori*” Fm; where present, foliation wraps the tourmaline spots (Fig. 4a). The contacts  
200 with the country rocks are usually tectonized and are locally characterized by the occurrence of  
201 breccias and/or by the comminution of the grain size, resulting in a blackening of the rock, as  
202 observed, for instance, along the border of the rock body occurring at Le Casette (Fig. 3e).  
203 Moreover, around the Fornovolasco Metarhyolite rock bodies, the metagreywackes and phyllites  
204 belonging to the “*Filladi inferiori*” Fm are distinctly tourmalinized and tourmaline veins, up to 1  
205 cm in thickness, cut the Fornovolasco Metarhyolite Fm itself (Fig. 3d). Usually, in the  
206 tourmalinized outcrops, the occurrence of thallium-bearing pyrite veins, associated with minor

207 arsenopyrite and trace amounts of other sulfides and sulfosalts (e.g., galena, tetrahedrite) has been  
208 observed (e.g., in the Boscaccio area – Fig. 3f).

209 The largest outcrops of this formation occur in the Fornovolasco tectonic window, whereas  
210 small and scattered outcrops are present in the Stazzemese area and in the Sant’Anna tectonic  
211 window (Fig. 2). As reported by Pieruccioni et al. (2018), the largest rock body is exposed close to  
212 Fornovolasco, in the Boscaccio locality, where it forms a lensoidal body of ca. 1.5 km in length and  
213 120 m in apparent thickness. Another significant outcrop was described by Bonatti (1933), close to  
214 Le Casette locality.

215 The bodies of these porphyritic rocks are usually flattened on the main field composite  
216 foliation. In the Fornovolasco area, this foliation records Alpine D1 and D2 events as well as pre-  
217 Alpine deformation (Variscan in age), as widely reported elsewhere in the Paleozoic basement of  
218 Alpi Apuane (e.g., Conti et al., 1991). Only locally, e.g., at Le Casette and Boscaccio, porphyritic  
219 rock bodies can be observed discordantly cutting the foliation (Variscan ?), which is crenulated and  
220 transposed in the Alpine main foliation far from the porphyritic body (Fig. 5b).

221

#### 222 *4.2. Petrography and mineral chemistry*

223

224 The Fornovolasco metarhyolite is characterized by a porphyritic texture (Figg. 4b-c, 6), with  
225 quartz, mica, and feldspar phenocrysts set in a fine-grained quartz-white mica-feldspar groundmass.  
226 Some samples are foliated, with porphyroclasts of quartz, tourmaline, and feldspar, wrapped by the  
227 foliation (Fig. 6c). Tectonic deformation may result in a reduction of the grain size, as observed in  
228 the blackened variety of metarhyolite found in the marginal portions of the outcrop of Le Casette.

229 Quartz is usually represented by anhedral to subhedral grains, up to 5 mm in size, sometimes  
230 showing rounded embayment structures (Fig. 6d). Euhedral hexagonal crystals sections have been  
231 also observed (Fig. 6e). Usually, such crystals display the formation of subgrain boundaries and  
232 undulose extinction, indicating their metamorphic recrystallization.

233 Feldspars occur both as albite (containing less than 0.01 K atoms per formula unit) and K-  
234 feldspar (Or<sub>97</sub>Ab<sub>3</sub>). They occur as subhedral prismatic crystals, up to 5 mm, usually partly or  
235 entirely replaced by fine-grained white mica. Albite and Albite-Carlsbad twins can be observed  
236 (Fig. 6f).

237 Phyllosilicates are represented by biotite, chlorite, and white mica (Table 2). Biotite is a  
238 relict igneous mineral and it is only rarely preserved (Fig. 6g), usually being replaced by an  
239 assemblage made of chlorite + quartz ± rutile, sometimes with inclusions of zircon, apatite, and  
240 ilmenite. Taking into account its average chemical composition,  
241  $K_{0.89}(Fe_{1.53}Mg_{1.00}Ti_{0.16}Al_{0.15}V_{0.02})_{\Sigma 2.86}(Al_{1.14}Si_{2.86})O_{10}(OH_{1.97}F_{0.03})$ , it can be classified as a Mg-rich  
242 annite (Rieder et al., 1998; Tischendorf et al., 2007). Chlorite, occurring in samples FVb7 (after  
243 biotite) and SAS1 (both after biotite and as synkinematic porphyroblasts aligned on the main field  
244 composite schistosity), has an average chemical composition  
245  $(Mg_{2.45}Fe_{2.22}Mn_{0.02}Al_{1.30}Ti_{0.01})(Si_{2.70}Al_{1.30})O_{10}(OH)_8$ , corresponding to a Fe-rich clinocllore  
246 (Wiewióra and Weiss, 1990).

247 White mica usually occurs as subhedral crystals showing a decussate texture; it can also  
248 form fine-grained individuals, closely associated with quartz and minor feldspar. On the basis of its  
249 chemistry, it can be classified as muscovite (Rieder et al., 1998; Tischendorf et al., 2007). Back-  
250 scattered electron images show a distinct chemical zoning, with dark and bright regions. This  
251 zoning is mainly related to the phengitic substitution. Only a minor paragonitic component was  
252 observed.

253 Tourmaline is widespread in almost all the studied samples, even if its modal abundance is  
254 highly variable. Tourmaline occurs as subhedral to anhedral grains, scattered within the  
255 groundmass, or as rounded spots, formed by the intimate intergrowth of tourmaline, quartz, and  
256 minor albite. In the more deformed samples, tourmaline crystals are strongly fractured, with  
257 fractures filled by quartz, and the tourmaline + quartz ± albite spots are wrapped by foliation.  
258 Optically, tourmaline crystals are zoned and strongly pleochroic, with green-bluish cores and brown

259 to tan rims (Fig. 6h). Such an optical zoning is related to a fine-scale oscillatory chemical zoning  
 260 revealed through SEM observations. The cation proportions of tourmaline from the Fornovolasco  
 261 metarhyolite are plotted in the Al–Fe(tot)–Mg and Ca–Fe(tot)–Mg ternary diagrams of Henry and  
 262 Guidotti (1985) (Fig. 7), whereas selected chemical analyses of tourmaline, representative of the  
 263 observed chemical variations, are given in Table 3. Following the nomenclature of Henry et al.  
 264 (2011), tourmalines occurring in the studied samples are members of the dravite-schorl series. Since  
 265 accurate determinations of B, O, H, Li are lacking, and the oxidation states of transition elements  
 266 are unknown, the chemical formulae were recalculated on the basis of 31 anions, assuming the  
 267 occurrence of 3 B and 4 OH groups per formula unit (i.e., on the basis of 24.5 O atoms, in  
 268 agreement with Henry et al., 2011). The total number of X and Y cations falls in the ranges  $X = 0.60$   
 269  $- 0.99$  atoms per formula unit (apfu) and  $Y = 2.71 - 2.98$  apfu. The occurrence of X vacancies  
 270 agrees with the alkali-defect substitution  $^X\text{Na}^+ + ^Y(\text{Mg}, \text{Fe})^{2+} = ^X\Box + ^Y\text{Al}^{3+}$ . Moreover, minor Ca  
 271 occurs as X cation, according to the uvite substitution  $^X\text{Na}^+ + ^Z\text{Al}^{3+} = ^X\text{Ca}^{2+} + ^Z(\text{Mg}, \text{Fe})^{2+}$ . The Y  
 272 vacancy may be interpreted in two different ways, owing to the lack of a complete analysis of  
 273 tourmaline. Indeed, the vacancy could be apparent, and related to a small oxy-component, with  
 274 minor (OH)<sup>−</sup> replaced by O<sup>2−</sup>, as suggested by Benvenuti et al. (1991) for tourmaline from the  
 275 Bottino mine (Alpi Apuane), or it could be real, in agreement with some structural refinements  
 276 showing small numbers of vacancies at both Y and Z sites (e.g., Ertl et al., 2003; Prowatke et al.,  
 277 2003). The Y cations are mainly represented by Mg and Fe, with Mg/(Mg + Fe) atomic ratio ranging  
 278 between 0.30 and 0.96. Magnesium and Fe can be replaced by Al, up to ~ 0.80 apfu. Titanium is  
 279 another minor substituent of Fe and Mg as Y cation, according to the substitution  $^Y(\text{Mg}, \text{Fe})^{2+} +$   
 280  $^T_2\text{Si}^{4+} = ^Y\text{Ti}^{4+} + ^T_2\text{Al}^{3+}$ ; Ti content up to ~ 0.60 apfu have been measured. The Z cation is mainly  
 281 represented by Al, even if the occurrence of minor Mg, related to the uvite substitution, cannot be  
 282 excluded. Finally, the T cations are represented by Si (in the range ~ 5.70 – 6.00 apfu) and minor  
 283 Al. The chemical analyses of tourmaline were performed on samples FVb7 (showing the best  
 284 preserved magmatic texture, with biotite relicts) and FVb9. It is worth noting that while tourmaline

285 in sample FVb7 has a rather homogeneous Mg/(Mg + Fe) atomic ratio [average = 0.50(4); range =  
286 0.44-0.58], sample FVb9 show more variability in Mg and Fe content, with an average Mg/(Mg +  
287 Fe) atomic ratio of 0.71(19), ranging from 0.30 to 0.96.

288 Accessory minerals are represented by apatite, epidote, monazite-(Ce) (in some cases  
289 included in apatite), rutile (usually after biotite), titanite, and zircon. Minor amounts of sulfides  
290 (pyrite, arsenopyrite, and traces of galena and tetrahedrite) have been observed in some samples.

291

### 292 4.3. Geochemistry

293

294 The studied rocks plot into the rhyolite field of the Total Alkali vs Silica classification  
295 diagram (Le Bas et al., 1986; Fig. 8a) and into the dacite/rhyodacite and trachyandesite fields of the  
296 Zr/TiO<sub>2</sub> vs Nb/Y diagram (Winchester and Floyd 1977; Fig. 8b). Having to choose between  
297 metarhyolite and metadacite/metarhyodacite/metatrachyandesite, we opted for metarhyolite to  
298 emphasize the SiO<sub>2</sub>- and quartz phenocryst-rich nature of studied rocks. The Fornovolasco  
299 metarhyolite is peraluminous having an Alumina Saturation Index (ASI) variable between 1.3 and  
300 3.2. The trace-element signature of these rocks is that typical of highly evolved orogenic magmas  
301 showing negative anomalies of Nb, Ta, P, and Ti in the Primitive Mantle-normalized patterns (Tab.  
302 4, Fig. 9a). The relative concentrations of Nb, Y, and Zr, that should be close to the original ones,  
303 even following moderate alteration and low-grade metamorphism (e.g., Pearce et al., 1984), are also  
304 indicative of an orogenic signature. The low contents of Sr and Ba, coupled with the negative Eu  
305 anomalies (Eu/Eu\* = 0.52-0.85; Fig. 9a, b) suggest extensive feldspar fractionation.

306 With respect to the felsic metavolcanic rocks (metarhyolite and metadacite; Fig. 8a) of the  
307 "*Porfiroidi e scisti porfirici*" Fm, the Fornovolasco metarhyolite has similar incompatible trace  
308 element distribution, systematically lower Zr, Hf, Y, Nb, Ba, Th and REE, and slightly higher  
309 LREE/HREE ratios (Fig. 9a, b). The moderate geochemical differences between the two rock suites  
310 could be either primary (magmatic) or due to the metamorphic/hydrothermal processes suffered by

311 the rocks. It is worth noting that some samples from Fornovolasco (e.g., FVb1, FVb13, and FVc2)  
312 show high enrichments in Pb, Bi, As, and Sb (Fig. 9a, Tab. 4).

313

#### 314 4.4. *U-Pb zircon age*

315

316 The LA-ICP-MS U-Pb analyses were performed on the four selected samples, representative of  
317 the main outcrops of the Fornovolasco Metarhyolite Fm in southern Alpi Apuane. Selected zircon  
318 crystals are generally euhedral and range in length between 100 and 300  $\mu\text{m}$ . Most of them have an  
319 elongated prismatic habit, with a width-to-length ratio  $> 2$  ( $\sim 81\%$ ), even if equant crystals occur ( $\sim$   
320  $19\%$ ). Some crystals contain fluid inclusions or mineral grains. The SEM-CL images (Fig. 10)  
321 revealed a complex internal structure. Usually, zircon crystals show a well-developed oscillatory  
322 zoning. About 28% of zircon crystals show structureless xenocrystic cores, even if some cores  
323 characterized by oscillatory or sector zoning have been observed; in some cases, faint oscillatory  
324 zoning can be distinguished. The following results have been obtained (all errors are given at the  $2\sigma$   
325 level):

326 **FVb13** – A total of 116 zircons were chosen. Among them, 90 have an elongated prismatic  
327 habit. SEM-CL images show the presence of 32 cores. A total of 122 LA spots on 82 zircons gave  
328 46 (36 rims + 10 cores) U-Pb concordant ages, varying between  $242 \pm 4$  to  $301 \pm 5$  Ma ( $^{206}\text{Pb}/^{238}\text{U}$   
329 ages). Core ages varied from  $260 \pm 7$  Ma to  $298 \pm 4$  Ma. Weighted average ages for rims and cores  
330 are  $271 \pm 4$  and  $277 \pm 9$  Ma, respectively.

331 **FVc1** – A total of 80 zircons was selected. Most of them show an elongated prismatic habit  
332 (61). SEM-CL images show the occurrence of 22 cores. A total of 85 LA spots on 61 zircons gave  
333 47 (40 rims + 7 cores) U-Pb concordant ages, with rim and core ages varying from  $256 \pm 6$  to  $296 \pm$   
334  $4$  Ma and from  $270 \pm 6$  to  $294 \pm 6$  Ma ( $^{206}\text{Pb}/^{238}\text{U}$  ages), respectively. Weighted average ages range  
335 between  $280 \pm 3$  Ma (rims) and  $283 \pm 7$  Ma (cores).

336 **POL1** – A total of 107 zircons were selected; 85 of them have an elongated prismatic habit.  
337 SEM-CL images show the occurrence of 33 cores. A total of 73 LA spots were performed on 55  
338 zircons, giving 24 U-Pb concordant ages (only on rims) varying between  $226 \pm 6$  and  $306 \pm 6$  Ma  
339 ( $^{206}\text{Pb}/^{238}\text{U}$  ages). The weighted average age is  $277 \pm 8$  Ma.

340 **SAS1** – A total of 114 zircons were chosen, 97 showing an elongated prismatic habit. SEM-CL  
341 images show the presence of 29 cores. A total of 106 LA spots, performed on 80 zircons, gave 52  
342 (44 rims + 8 cores) U-Pb concordant ages, varying between  $259 \pm 7$  to  $311 \pm 5$  Ma ( $^{206}\text{Pb}/^{238}\text{U}$   
343 ages), with core ages varying from  $281 \pm 5$  Ma to  $301 \pm 5$  Ma. Weighted average ages on cores and  
344 rims are  $290 \pm 6$  and  $292 \pm 3$  Ma, respectively.

345 Table 5 and Figures 11 and 12 summarize such results. A total of 386 LA spots have been  
346 collected on 278 different zircon crystals of the Fornovolasco metarhyolite. They gave 169 U-Pb  
347 concordant ages (Fig. 11), having a weighted average age of  $280 \pm 2$  Ma. However, the probability  
348 density plot estimation reported in Figure 11 does not show a simple Gaussian distribution,  
349 suggesting the contribution of at least two different populations, plus few occurrences at younger  
350 ages. The main population could resolve an event occurring at the modal value ( $\sim 288$  Ma), whereas  
351 a second event could be represented by relatively younger ages (at  $\sim 270$  Ma).

352 Figure 12 shows the different age distributions for the four studied samples. Samples FVc1 and  
353 SAS1 have the higher percentage of concordant data (55% and 49%, respectively), whereas FVb13  
354 and POL1 have only 38% and 33% of concordant data, respectively. The 217 discordant ages were  
355 excluded. Among the U-Pb concordant ages, 164 data indicate an age spread over a 50 Ma period,  
356 from late Carboniferous to middle Permian (Figure 12). The remaining five concordant data,  
357 belonging to samples FVb13 and POL1, gave younger ages, ranging from  $226 \pm 6$  to  $244 \pm 9$  Ma.

358

## 359 **5. Discussion**

360

### 361 *5.1. The Fornovolasco metarhyolite: a Permian magmatic product*

362

363        Previous authors debated the nature of the porphyritic tourmaline-rich rocks of the southern  
364    Alpi Apuane, assigning them different origins (e.g., Bonatti, 1933). Pandeli et al. (2004), on the  
365    basis of petrographic features, described such rocks as metavolcanic products. The textural and  
366    mineralogical features observed in all the studied samples (Table 1), representative of the different  
367    outcrops of the Fornovolasco Metarhyolite Fm, support their magmatic origin. Indeed, they show a  
368    porphyritic texture, with euhedral phenocrysts of feldspar and quartz, the latter with embayment  
369    structures, coupled with the occurrence of relict femic phases (e.g., biotite), tourmaline spots, and  
370    zircon crystals showing magmatic *habitus* (Figg. 3, 4, 6, 10).

371        The Alpine tectono-metamorphic overprint partially obliterated the original petrographic  
372    features of these rocks. In addition, the widespread tourmalinization and the local occurrence of  
373    pyrite veins (Fig. 3d, f) suggest that these rocks had been affected by hydrothermal processes with  
374    an additional possible alteration of the original compositional and textural characteristics. As a  
375    matter of fact, it is well-known that the selective alteration and deformation of felsic igneous rocks  
376    in hydrothermal-metamorphic conditions could result in rocks mainly formed by quartz and white  
377    mica (e.g., Etheridge and Vernon, 1981; Williams and Burr, 1994; Vernon, 2004), with only a few  
378    relicts of the more alterable phases (e.g., feldspar, biotite). The Fornovolasco metarhyolite shows  
379    variable textures, from well-preserved porphyritic ones, with relict biotite, feldspar, and embayed  
380    magmatic quartz still preserved (Fig. 6), to strongly deformed rocks, where the magmatic texture  
381    was partially to completely obliterated.

382        Notwithstanding such alteration and deformation processes, the structural as well as the  
383    petrographic data support a subvolcanic setting for the Fornovolasco metarhyolite. For instance, the  
384    study of the field relationships between some metarhyolite bodies and the foliation of the  
385    surrounding schists (Fig. 5) suggests that these rocks originally emplaced as dykes or laccoliths. A  
386    subvolcanic nature is also supported by the occurrence of tourmaline spots and agrees with the  
387    textural features of the Fornovolasco Metarhyolite (e.g., porphyritic texture, embayed quartz – Figg.



388 3, 6). Indeed, tourmaline spots are a distinctive feature mostly occurring in leucocratic intrusive  
389 rocks (e.g., Buriánek and Novák, 2007; Perugini and Poli, 2007; Hong et al., 2017 and references  
390 therein); even if their origin is still debated, they are usually related to an intrusive or subvolcanic  
391 magmatic-hydrothermal setting. The formation of the tourmaline spots clearly predates the Alpine  
392 tectono-metamorphic events, being wrapped by the Alpine foliation (when the latter is developed  
393 within strongly deformed horizons in the metarhyolite rock bodies – Fig. 4a).

394 As stated above, the U-Pb concordant ages extend over a time interval of about 50 Ma, from  
395 late Carboniferous to middle Permian. Such a spread is common to the four studied samples,  
396 although every one displays a different age distribution within this interval (Fig. 12). It is worth  
397 noting that such a variability is common to several Permian magmatic rocks throughout Europe  
398 (e.g., Cortesogno et al., 1998; Finger et al., 2003; Visonà et al., 2007; Dallagiovanna et al., 2009).  
399 Owing to the general homogeneity of the petrographical and geochemical features of the  
400 Fornovolasco metarhyolite occurring over the studied area, a single magmatic event could be  
401 hypothesized. Taking into account the U-Pb ages and their weighted averages (Table 5), an early-  
402 middle Permian age can be proposed, fitting with the regional framework (Fig. 13) showing the  
403 occurrence of sedimentary basins, as testified by the *Scisti di San Lorenzo* and *Rio Marina* Fms  
404 (dated at 280 Ma – Siirevaag et al., 2016; Paoli et al., 2017), as well as a thermal event, recorded in  
405 the *Filladi di Buti* Fm (Monti Pisani) and in the *Micascisti* Fm in the Larderello sub-surface and  
406 dated between 275 and 285 Ma (Borsi et al., 1966; Del Moro et al., 1982; Ferrara and Tonarini,  
407 1985). Moreover, it agrees with the ages of several peraluminous felsic and minor mafic magmatic  
408 bodies emplaced during the post-Variscan extensional phase in the southern sector of the Variscan  
409 belt in Western Europe (e.g., Stampfli and Borel, 2002; Stampfli et al., 2002; Schuster and Stüwe,  
410 2008; von Raumer et al., 2016). The probability density distribution of zircon ages showing two  
411 different zircon populations reported in Fig. 11 could be interpreted as the result of an early  
412 magmatic crystallization (at ~ 288 Ma), corresponding to the modal value, and a subsequent post-  
413 magmatic event affecting the original U-Pb zircon systematics leading to younger ages (e.g.,

414 Bomparola et al., 2007). The nature of this event is presently not known, even if it could be  
415 hypothetically related to hydrothermal alteration and sulfide deposition, occurring in some of these  
416 rock bodies and geochemically expressed as high contents As, Sb, Pb, and Bi (Fig. 9, Table 4). The  
417 second population of ages is particularly frequent in samples FVb13 and POL1, having zircon  
418 showing younger ages and the lower percentage of concordant data. Such younger ages agree with  
419 the results obtained by Molli et al. (2002) on amphiboles from the Cerreto metamorphic slices  
420 (northern Alpi Apuane), that showed a late Permian – early Triassic overprint (~ 240 Ma) possibly  
421 related by these authors to the Variscan orogenic collapse or the Tethyan rift-related crustal  
422 thinning.

423 An alternative interpretation of the time spread shown by the data (Figg. 11, 12) could be that  
424 the older concordant ages, ranging between 275 and 310 Ma, measured on xenocrystic and  
425 oscillatory-zoned cores and rims, are due to inherited components from the source rocks, whereas  
426 the age of the magmatic event could range between 260 and 275 Ma, as resulting from the youngest  
427  $^{206}\text{Pb}/^{238}\text{U}$  ages measured on oscillatory zoned rims. This interpretation agrees with the results of  
428 Dallagiovanna et al. (2009), who found inherited cores only slightly older than the magmatic rims.

429 Further studies are needed to propose a clear picture of the Permian magmatism recorded in the  
430 Alpi Apuane Metamorphic Complex. As a matter of fact, the Fornovolasco metarhyolite represents  
431 the record of a magmatic event following the Variscan orogeny and gives new hints on the Permian  
432 evolution of the basement of the Adria plate.

433

## 434 5.2. The Variscan magmatism in Northern Apennines

435

436 The occurrence of a late- to post-Variscan magmatism in the Northern Apennines was  
437 hypothesized by several authors through the identification of metavolcanoclastic Permian  
438 formations in some of the small and scattered outcrops of Paleozoic rocks occurring in Tuscany  
439 (Fig. 13). For instance, the “*Scisti porfirici di Iano*” Fm (central Tuscany) is made of rhyolitic

440 metavolcaniclastic rocks (e.g., Barberi, 1966; Lazzarotto et al., 2003 and references therein), and  
441 abundant fragments of volcanic rocks have been found in the “*Arenarie rosse di Castelnuovo*” Fm,  
442 known in the Larderello subsurface (southern Tuscany; Bagnoli et al., 1979) and in the AGIP  
443 “Pontremoli 1” well (northern Tuscany; Pandeli et al., 1994). It is worth noting that the Permian age  
444 attribution is only based on stratigraphic correlations. Moreover, pebbles of red rhyolitic porphyries,  
445 similar to the Permian rhyolites from southern Alps and Sardinia, were found in the Middle Triassic  
446 Verruca Fm of the Monti Pisani (northern Tuscany) (e.g., Puxeddu et al., 1984). Finally, several  
447 megaliths of granitoid rocks occurring in the External Liguride units have been interpreted as  
448 fragments of the continental crust partially derived from the Adria plate margin. Their ages,  
449 obtained by Eberhardt et al. (1962) through K/Ar and Rb/Sr dating on muscovite, range between  
450  $272 \pm 16$  and  $310 \pm 10$  Ma.

451 The age of the Variscan and post-Variscan metamorphism in the basement of the Northern  
452 Apennines was dated by several authors. Molli et al. (2002) reported  $^{40}\text{Ar}/^{39}\text{Ar}$  ages measured on  
453 amphibole of 328 – 312 Ma for the MORB-derived ortho-amphibolites of the Cerreto metamorphic  
454 slices, whereas Lo Pò et al. (2016), on the basis of the chemical dating of monazite, suggested a  
455 metamorphic peak at  $292.9 \pm 3$  Ma for the metasedimentary rocks recovered in the “Pontremoli 1”  
456 well. The occurrence of a post-Variscan high-*T* thermal event was previously suggested by Del  
457 Moro et al. (1982), on the basis of a Rb/Sr age of  $285 \pm 11$  Ma obtained for muscovite associated  
458 with andalusite in the “*Micasisti*” Fm in the Larderello subsurface. Such an age is similar to those  
459 found using Rb/Sr dating on whole rock for the “*Filladi e Quarziti di Buti*” Fm (Monti Pisani), i.e.,  
460  $285 \pm 12$  Ma (Borsi et al., 1966; Ferrara and Tonarini, 1985). Consequently, this formation, recently  
461 dated through U-Pb zircon dating to the late Proterozoic – early Cambrian by Paoli et al. (2017),  
462 possibly recorded also an early-middle Permian metamorphism.

463 The thermal events recorded in the Paleozoic basement could be related to the thinning of the  
464 lithosphere and the emplacement of magmatic bodies following the Variscan orogeny, e.g., gabbro-  
465 derived granulites from the External Liguride Units having Sm/Nd ages of  $\sim 290$  Ma obtained on

466 clinopyroxene, plagioclase, and whole rock (Marroni and Tribuzio, 1996; Meli et al., 1996; Marroni  
467 et al., 1998; Montanini and Tribuzio, 2001). This evidence agrees with the dating of the  
468 Fornovolasco metarhyolite, that can be considered as the first evidence of Permian subvolcanic  
469 magmatic bodies intruded in the Paleozoic basement of the Northern Apennines.

470

### 471 *5.3. Permian magmatism and ore genesis in the Alpi Apuane*

472

473 As pointed above, the Fornovolasco metarhyolite is spatially associated with the main ore  
474 deposits from the southern Alpi Apuane (Fig. 2), as well as to tourmalinite bodies. Moreover, the  
475 widespread occurrence of tourmaline in the metarhyolite is a distinctive feature (Fig. 3).

476 The occurrence of tourmalinite in the Paleozoic basement of the southern Alpi Apuane has  
477 been known since a long time and was used by miners as an empirical prospecting tool (e.g.,  
478 Benvenuti et al., 1989). Several origins have been proposed for such a rock: magmatic (D'Achiardi,  
479 1885), magmatic-hydrothermal, related to a hypothetical Tertiary magmatism (Carmignani et al.,  
480 1972, 1975), and sedimentary-exhalative (Benvenuti et al., 1989). According to these latter authors,  
481 the occurrence of tourmalinite could indicate a pre-Alpine concentration of boron and metals, later  
482 remobilized during the Alpine tectono-metamorphic events. Indeed, several authors proposed a  
483 genetic link between tourmalinite and ore deposits (e.g., Lattanzi et al., 1994 and references  
484 therein). As a consequence, the age of the tourmalinization event has been taken as the age of the  
485 proto-ores. Following Benvenuti et al. (1989), an early Paleozoic age for the tourmalinization  
486 process was suggested, related to the middle Ordovician “*Porfiroidi*” magmatic cycle, even if such  
487 an age was attributed only to the Pb-Zn-Ag ore bodies. On the contrary, a possible Permo-Triassic  
488 age was suggested for the pyrite  $\pm$  baryte  $\pm$  iron oxide ore deposits and the associated tourmalinite  
489 (e.g., Costagliola et al., 1990). Finally, D’Orazio et al. (2017), based on their identical Pb-isotope  
490 composition, proposed a common early Paleozoic origin for all the major Pb-Zn-Ag and pyrite  $\pm$   
491 baryte  $\pm$  iron oxide deposits from the southern Alpi Apuane.

492 The discovery of a Permian magmatism in this area allows refining this minerogenetic model.  
493 Indeed, tourmalinization seems to be related to the occurrence of the metarhyolite bodies, in  
494 agreement with the usual association of tourmaline + quartz hydrothermal veins and metasomatic  
495 bodies with shallow crustal level tourmaline-bearing felsic rocks (e.g., Dini et al., 2008). Moreover,  
496 lead isotope composition obtained for sulfides and sulfosalts from the ore deposits of southern Alpi  
497 Apuane is similar to that shown by the ores generated during the Paleozoic metallogenetic event of  
498 Sardinia and its Variscan magmatic rocks (D'Orazio et al., 2017). The lack of knowledge about the  
499 occurrence of a Permian magmatism led these authors to hypothesize a genetic link with the middle  
500 Ordovician magmatism. On the contrary, the present study allows discarding this hypothesis,  
501 suggesting a Permian age for the major ore deposits from southern Alpi Apuane. It is worth noting  
502 that the geochemistry of these pyrite ores is typical of low-*T* hydrothermal systems, in some cases  
503 associated with a coeval felsic magmatism occurring in an evolved continental crust (e.g., Lentz,  
504 1998). It is very likely that the study area was characterized by a similar geodynamic setting in post-  
505 Variscan time, in agreement with several authors (e.g., Rau, 1990; Marroni et al., 1998; Padovano et  
506 al., 2012; Lo Pò et al., 2016).

507 A pre-Ladinian tourmalinization event was suggested by Cavarretta et al. (1989, 1992), owing  
508 to the occurrence of tourmalinite clasts within the Middle Triassic metasiliciclastic Verrucano  
509 sequence. These authors hypothesized a Permian high-*T* hydrothermal activity, associated with acid  
510 magmatism, related to the extensional phase of the Variscan orogeny. Moreover, on the basis of the  
511 crystal chemistry of tourmaline in the tourmalinite clasts, Cavarretta et al. (1989, 1992) proposed an  
512 exhalative origin for tourmaline, with the interaction between magmatic fluids and Mg-rich cold  
513 seawater. A similar hypothesis was put forward by Benvenuti et al. (1991) for tourmaline from the  
514 Bottino mine (southern Alpi Apuane).

515 Tourmaline from both metarhyolite bodies and tourmalinite has a variable chemistry within the  
516 schorl-dravite series, with a wide range of Mg/(Mg+Fe) atomic ratios, as shown in Fig. 7. In  
517 particular, the chemical composition of tourmaline in sample FVb7, forming the typical black spots,

518 is more iron-rich and homogeneous and it is similar to those reported by Benvenuti et al. (1991) for  
519 tourmaline from tourmalinite bodies. On the contrary, tourmaline occurring in sample FVb9,  
520 scattered in the groundmass, has a wide compositional range, from Fe-rich to Mg-rich composition.

521 The close similarity between the chemistry of tourmaline from metarhyolite bodies and  
522 tourmalinite could suggest their common origin, likely related to hydrothermal circulation. It is  
523 well-known that no specific compositional field can be established in the diagrams of Henry and  
524 Guidotti (1985) for tourmaline from tourmalinites, owing to their wide compositional range (e.g.,  
525 Plimer and Lees, 1988; Slack, 1996; Torres-Ruiz et al., 2003). Indeed, tourmaline from the  
526 Fornovolasco metarhyolite falls in the compositional fields corresponding to clastic metasediments,  
527 Li-poor granitoids, and Fe<sup>3+</sup>-rich quartz-tourmaline rocks, in agreement with occurrences from  
528 other localities worldwide (e.g., tourmaline in tourmalinites from the Betic Cordillera, Spain –  
529 Torres-Ruiz et al., 2003). Consequently, the diagram of Henry and Guidotti (1985) can be used only  
530 to illustrate the wide chemical variability of tourmaline from the Fornovolasco metarhyolite,  
531 avoiding any petrogenetic implication. It is worth noting that such compositional variations likely  
532 reflect the pre-metamorphic magmatic-hydrothermal as well as syn- to post-metamorphic processes  
533 affecting the basement of the Alpi Apuane, and constitute an essential tile in the reconstruction of  
534 the genesis of ore deposits (e.g., Slack, 1996 and references therein). Consequently, a more detailed  
535 study of the chemical and isotopic composition of tourmaline seems to be mandatory.

536

## 537 **6. Summary and conclusion**

538

539 The data reported in this work document that the Fornovolasco metarhyolite is the first  
540 occurrence of Permian felsic magmatic rocks within the basement of Northern Apennines, where  
541 only metavolcanoclastic rocks were known in Permo-Triassic metasediments. This finding fits with  
542 the previous knowledge in other sectors of the West-Mediterranean southern Europe, such as  
543 Eastern and Southern Alps, Ligurian Alps; Corsica, Sardinia, and Calabria (e.g., Dal Piaz, 1993;

544 Cortesogno et al., 1998; Visonà et al., 2007; Schuster and Stüwe, 2008; Dallagiovanna et al., 2009;  
545 Festa et al., 2010; Oggiano et al., 2010; Zibra et al., 2010). The Fornovolasco metarhyolite shares  
546 its calc-alkaline nature with the late Carboniferous to early Permian magmatic products occurring in  
547 these areas and referred to a generalized lithospheric thinning associated with a regional-scale  
548 crustal wrenching (e.g., Deroin and Bonin, 2003; Dallagiovanna et al., 2009 and references therein).  
549 The discovery of Permian magmatic rocks within the basement of the Northern Apennines gives  
550 new hints for a better knowledge and understanding of the geodynamic evolution of the  
551 “Apenninic” portions of the Adria plate basement. Moreover, it fits the results of previous studies  
552 on the Northern Apennine basement, showing the occurrence of a post-Variscan thermal event  
553 recorded in the basement rocks at Permian time, hypothetically related to the thinning of the  
554 lithosphere and the emplacement of magmatic bodies. Finally, the finding of Permian magmatic  
555 rocks in close spatial association with the ore deposits of the Alpi Apuane Metamorphic Complex  
556 represents a significant constraint on the origin and age of these ores.

557

## 558 **Acknowledgements**

559

560 This research received support by Ministero dell'Istruzione, dell'Università e della Ricerca  
561 through the project SIR 2014 “THALMIGEN – Thallium: Mineralogy, Geochemistry, and  
562 Environmental Hazards” (Grant No. RBSI14A1CV), granted to CB. MP wish to acknowledge the  
563 European Research Council for the Consolidator grant CHRONOS (Grant No. 612776 – P.I. Diego  
564 Perugini). The constructive criticism of two anonymous reviewers helped us improving the paper.

565

566

567   **References**

568

569   Bagnoli, G., Tongiorgi, M., 1980. New Silurian fossiliferous (Mt. Corchia) and Devonian  
570       (Monticiano) layers in the Tuscan Paleozoic. *Memorie della Società Geologica Italiana* 20,  
571       301-313.

572   Bagnoli, G., Gianelli, G., Puxeddu, M., Rau, A., Squarci, P., Tongiorgi, M., 1979. A tentative  
573       stratigraphic reconstruction of the Tuscan Paleozoic basement. *Memorie della Società*  
574       *Geologica Italiana* 20, 99-116.

575   Barberi, F., 1966. I porfiroidi della Toscana e la loro posizione stratigrafica. *Atti del Symposium sul*  
576       *Verrucano, Pisa, settembre 1965. Società Toscana di Scienze Naturali, Pisa*, 34-53.

577   Barberi, F., Giglia, G., 1965. La serie scistosa basale dell'Autoctono delle Alpi Apuane. *Bollettino*  
578       *della Società Geologica Italiana* 84, 41-92.

579   Benvenuti, M., Lattanzi, P., Tanelli, G., 1989. Tourmalinite-associated Pb-Zn-Ag mineralization at  
580       Bottino, Apuane Alps, Italy: geologic setting, mineral textures, and sulfide chemistry.  
581       *Economic Geology* 84, 1277-1292.

582   Benvenuti, M., Costagliola, P., Lattanzi, P., Tanelli, G., 1991. Mineral chemistry of tourmalines  
583       from the Bottino mining district, Apuane Alps (Italy). *European Journal of Mineralogy* 3,  
584       537-548.

585   Bomparola, R.M., Ghezzo, C., Belousova, E., Griffin, W.L., O'Reilly, S.Y. (2007) Resetting of the  
586       U-Pb zircon system in Cambro-Ordovician intrusives of the Deep Freeze Range, Northern  
587       Victoria Land, Antarctica. *Journal of Petrology* 48, 327-364.

588   Bonatti, S., 1933. La roccia porfiroide di Forno Volasco. *Atti della Società Toscana di Scienze*  
589       *Naturali, Memorie* 43, 210-216.

590   Bonatti, S., 1938. Studio petrografico delle Alpi Apuane. *Memorie descrittive della Carta Geologica*  
591       *d'Italia* 26, 116 p.



- 592 Borsi, S., Ferrara, G., Rau, A., Tongiorgi, M., 1966. Determinazioni col metodo Rb/Sr delle filladi e  
593 quarziti listate di Buti (Monti Pisani). Atti della Società Toscana di Scienze Naturali,  
594 Memorie 73, 632-646.
- 595 Buriánek, D., Novák, M., 2007. Compositional evolution and substitutions in disseminated and  
596 nodular tourmaline from leucocratic granites: Examples from the Bohemian Massif, Czech  
597 Republic. Lithos 95, 148-164.
- 598 Carmignani, L., Kligfield, R., 1990. Crustal extension in the Northern Apennines: the transition  
599 from compression to extension in the Alpi Apuane core complex. Tectonics 9, 1275-1303.
- 600 Carmignani, L., Dessau, G., Duchi, G., 1972. I giacimenti minerari delle Alpi Apuane e loro  
601 correlazioni con l'evoluzione del gruppo montuoso. Memorie della Società Geologica Italiana  
602 11, 417-431.
- 603 Carmignani, L., Dessau, G., Duchi, G., 1975. Una mineralizzazione sin-tettonica: il giacimento di  
604 Valdicastello (Alpi Apuane). Rapporti fra tettonica e minerogenesi in Toscana. Bollettino  
605 della Società Geologica Italiana 94, 725-758.
- 606 Carmignani, L., Dessau, G., Duchi, G., 1976. I giacimenti a barite, pirite e ossidi di ferro delle Alpi  
607 Apuane. Studio minerogenetico e strutturale. Nuove osservazioni sui giacimenti polimetallici.  
608 Bollettino della Società Geologica Italiana 95, 1009-1061.
- 609 Cavarretta, G., Puxeddu, M., Franceschelli, M., Pandeli, E., Valori, A., 1989. Tourmalinites from  
610 hydrothermal systems related to Permian rift magmatism of the Hercynian Saalian phase in  
611 Tuscany (Italy). In: D.L. Miles (Ed.) – Proceedings of the Sixth International Symposium  
612 Water-Rock interaction, Malvern (GB), 3-8 August, 1989, 141-144.
- 613 Cavarretta, G., Franceschelli, M., Pandeli, E., Puxeddu, M., Valori, A., 1992. Tourmalinites from  
614 the Triassic Verrucano of the Northern Apennines, Italy. In: L. Carmignani, F.P. Sassi (Eds.) -  
615 Contributions to the Geology of Italy with special regard to the Paleozoic basement. A  
616 volume dedicated to Tommaso Coccozza. IGCP 276, 335-338.

617 Conti, P., Di Pisa, A., Gattiglio, M., Meccheri, M., Vietti, N., 1988. Nuovi dati sulle metabasiti di  
 618 Valle del Giardino del basamento paleozoico apuano (Appennino settentrionale). Atti della  
 619 Società Toscana di Scienze Naturali, Memorie 95, 89-103.

620 Conti, P., Gattiglio, M., Meccheri, M., 1991. The overprint of the Alpine tectono-metamorphic  
 621 evolution on the Hercynian orogen: an example from the Apuane Alps (Northern Apennines,  
 622 Italy). Tectonophysics 191, 335-346.

623 Conti, P., Di Pisa, A., Gattiglio, M., Meccheri, M., 1993. The pre-Alpine basement in the Alpi  
 624 Apuane (Northern Apennines, Italy). In: von Raumer, J.F., Neubauer, F. (Eds.), Pre-Mesozoic  
 625 Geology in the Alps, Springer Verlag, Berlin, 609-621.

626 Conti, P., Carmignani, L., Meccheri, M., Massa, G., Fantozzi, P.L., Masetti, G., Rossetto, R., 2012.  
 627 Note illustrative della Carta Geologica d'Italia alla scala 1:50.000 "Foglio 206 – Viareggio".  
 628 Servizio Geologico d'Italia, Roma, 145 p.

629 Cortesogno, L., Cassinis, G., Dallagiovanna, G., Gaggero, L., Oggiano, G., Ronchi, A., Seno, S.,  
 630 Vanossi, M., 1998. The Variscan post-collisional volcanism in Late Carboniferous–Permian  
 631 sequences of Ligurian Alps, Southern Alps and Sardinia (Italy): a synthesis. Lithos 45, 305-  
 632 328.

633 Costagliola, P., Benvenuti, M., Tanelli, G., Cortecci, G., Lattanzi, P., 1990. The barite-pyrite-iron  
 634 oxides deposit of Monte Arsiccio (Apuane Alps). Geological setting, mineralogy, fluid  
 635 inclusions, stable isotopes and genesis. Bollettino della Società Geologica Italiana 109, 267-  
 636 277.

637 Cruciani, G., Franceschelli, M., Musumeci, G., Spano, M.E., Tiepolo, M., 2013. U-Pb zircon dating  
 638 and nature of metavolcanics and metarkoses from Monte Grighini Unit: new insights on Late  
 639 Ordovician magmatism in the Variscan belt in Sardinia, Italy. International Journal of Earth  
 640 Sciences 102, 2077-2096.

641 D'Achiardi, A., 1885. Tormalinolite del Bottino nelle Alpi Apuane. Atti della Società Toscana di  
 642 Scienze Naturali, Processi Verbalì 5, 204-207.

643 D'Orazio, M., Biagioni, C., Dini, A., Vezzoni, S., 2017. Thallium-rich pyrite ores from the Apuan  
644 Alps, Tuscany, Italy: constraints for their origin and environmental concerns. *Mineralium*  
645 *Deposita* 52, 687-707.

646 Dallagiovanna, G., Gaggero, L., Maino, M., Seno, S., Tiepolo, M., 2009. U-Pb zircon ages for post-  
647 Variscan volcanism in the Ligurian Alps (Northern Italy). *Journal of the Geological Society*,  
648 London, 166, 101-114.

649 Dal Piaz, G.V., 1993. Evolution of Austro-alpine and Upper Penninic basement in the North  
650 Western Alps from Variscan convergence to post-Variscan extension. In: von Raumer, J.E,  
651 Neubauer, E (Eds.), *Pre-Mesozoic Geology in the Alps*. Springer-Verlag, Berlin, pp. 327-344.

652 Del Moro, A., Puxeddu, M., Radicati di Brozolo, F., Villa, I.M., 1982. Rb-Sr and K-Ar ages on  
653 minerals at temperatures of 300°-400°C from deep wells in the Larderello geothermal field  
654 (Italy). *Contributions to Mineralogy and Petrology* 81, 340-349.

655 Derooin, J.P., Bonin, B., 2003. Late Variscan tectonomagmatic activity in western Europe and  
656 surrounding areas: The Mid-Permian episode: *Bollettino della Società Geologica Italiana*,  
657 Special Volume, 2, 169–184.

658 Di Pisa, A., Franceschelli, M., Leoni, L., Meccheri, M., 1985. Regional variation of the  
659 metamorphic temperatures across the Tuscanid I unit and its implications on the Alpine  
660 metamorphism (Apuan Alps, N. Tuscany). *Neues Jahrbuch für Mineralogie, Abhandlungen*  
661 151, 197-211.

662 Dini, A., Mazzarini, F., Musumeci, G., Rocchi, S., 2008. Multiple hydro-fracturing by boron-rich  
663 fluids in the Late Miocene contact aureole of eastern Elba Island (Tuscany, Italy). *Terra Nova*  
664 20, 318-326.

665 Eberhardt, P., Ferrara, G., Tongiorgi, E., 1962. Determination de l'âge des granites allochtones de  
666 l'Apennin septentrional. *Bulletin de la Société Géologique de France* 4, 666-667.

667 Ertl, A., Hughes, J.M., Prowatke, S., Rossman, G.R., London, D., Fritz, E.A., 2003. Mn-rich  
668 tourmaline from Austria: structure, chemistry, optical spectra, and relations to synthetic solid  
669 solutions. *American Mineralogist* 88, 1369-1376.

670 Etheridge, M.A., Vernon, R.H., 1981. A deformed polymictic conglomerate – the influence of grain  
671 size and composition on the mechanism and rate of deformation. *Tectonophysics* 79, 237-254.

672 Fellin, M.G., Reiners, P.W., Brandon, M.T., Wüthrich, E., Balestrieri, M.L., Molli, G., 2007.  
673 Thermochronologic evidence for the exhumation history of the Alpi Apuane metamorphic  
674 core complex, northern Apennines, Italy. *Tectonics* 26, TC6015.

675 ~~Fernández-Suárez, J., Arenas, R., Jeffries, T.E., Whitehouse, M.J., Villaseca, C., 2006. A U-Pb~~  
676 ~~study of zircons from a lower crustal granulite xenolith of the Spanish Central System: a~~  
677 ~~record of Iberian lithospheric evolution from the Neoproterozoic to the Triassic. *The Journal of*~~  
678 ~~*Geology* 114, 471-483.~~

679 Ferrara, G., Tonarini, S., 1985. Radiometric geochronology in Tuscany: results and problems.  
680 *Rendiconti della Società Italiana di Mineralogia e Petrologia* 40, 111-124.

681 Festa, V., Langone, A., Caggianelli, A., Rottura, A., 2010. Dike magmatism in the Sila Grande  
682 (Calabria, southern Italy): Evidence of Pennsylvanian–Early Permian exhumation. *Geosphere*;  
683 6(5) 549–566.

684 Finger, F., Broska, I., Haunschmid, B., Hrasko, L., Kohút, M., Krenn, E., Petrík, I., Riegler, G.,  
685 Uher, P., 2003. Electron-microprobe dating of monazites from Western Carpathian basement  
686 granitoids: Plutonic evidence for an important Permian rifting event subsequent to Variscan  
687 crustal anatexis. *International Journal of Earth Sciences* 92, 86-98.

688 Franceschelli, M., Leoni, L., Memmi, I., Puxeddu, M., 1986. Regional distribution of Al-silicates  
689 and metamorphic zonation in the low-grade Verrucano metasediments from the Northern  
690 Apennines, Italy. *Journal of Metamorphic Geology*, 4, 309-321.

691 Franceschelli, M., Gianelli, G., Pandeli, E., Puxeddu, M., 2004. Variscan and Alpine metamorphic  
692 events in the northern Apennines (Italy): a review. *Periodico di Mineralogia* 73, 43-56.

693 Gattiglio, M., Meccheri, M., Tongiorgi, M., 1989. Stratigraphic correlation forms of the Tuscan  
694 Paleozoic basement. *Rendiconti della Società Geologica Italiana* 12, 247-257.

695 Henry, D.J., Guidotti, C.V., 1985. Tourmaline as a petrogenetic indicator mineral: an example from  
696 the staurolite-grade metapelites of NW Maine. *American Mineralogist* 70, 1-15.

697 Henry, D.J., Novák, M., Hawthorne, F.C., Ertl, A., Dutrow, B.L., Uher, P., Pezzotta, F., 2011.  
698 Nomenclature of the tourmaline-supergroup minerals. *American Mineralogist* 96, 895-913.

699 Hong, W., Cooke, D.R., Zhang, L., Fox, N., Thompson, J., 2017. Tourmaline-rich features in the  
700 Heemskirk and Pierman Heads granites from western Tasmania, Australia: Characteristics,  
701 origins, and implications for tin mineralization. *American Mineralogist* 102, 876-899.

702 Jolivet, L., Faccenna, C., Goffé, B., Mattei, M., Rossetti, F., Brunet, C., Storti, F., Funiciello, R.,  
703 Cadet, J.P., D'Agostino, N., Parra, T., 1998. Midcrustal shear zones in postorogenic  
704 extension: Examples from the northern Tyrrhenian Sea. *Journal of Geophysical Research:*  
705 *Solid Earth* 103, 12123-12160.

706 Kroner, U., Romer R.L., 2013. Two plates – many subduction zones: the Variscan orogeny  
707 reconsidered. *Gondwana Research* 24, 298-329.

708 Lattanzi, P., Benvenuti, M., Costagliola, P., Tanelli, G., 1994. An overview on recent research on  
709 the metallogeny of Tuscany, with special reference to the Apuane Alps. *Memorie della*  
710 *Società Geologica Italiana* 48, 613-625.

711 Lazzarotto, A., Aldinucci, M., Cirilli, S., Costantini, A., Decandia, F.A., Pandeli, E., Sandrelli, F.,  
712 Spina, A., 2003. Stratigraphic correlation of the Upper Paleozoic – Triassic successions in  
713 southern Tuscany, Italy. *Bollettino della Società Geologica Italiana, Volume Speciale* 2, 25-  
714 35.

715 Le Bas, M.J., Le Maiter, W., Streckeisen, A., Zanettin, B., 1986. A chemical classification of  
716 volcanic rocks based on the Total Alkali-Silica diagram. *Journal of Petrology* 27, 745-750.

717 Lentz, D.R., 1998. Petrogenetic evolution of felsic volcanic sequences associated with Phanerozoic  
718 volcanic-hosted massive sulphide systems: the role of extensional geodynamics. *Ore Geology*  
719 *Reviews* 12, 289-327.

720 Lo Pò, D., Braga, R., Massonne, H.-J., Molli, G., Montanini, A., Theye, T., 2016. Fluid-induced  
721 breakdown of monazite in medium-grade metasedimentary rocks of the Pontremoli basement  
722 (Northern Apennines, Italy). *Journal of Metamorphic Geology* 34, 63-84.

723 London, D., Morgan, G.B.VI., Wolf, M.B., 1996. Boron in granitic rocks and their contact aureoles.  
724 *Reviews in Mineralogy and Geochemistry* 33, 299-330.

725 Lotti, B., 1882. Sulla separazione degli scisti triassici da quelli paleozoici nelle Alpi Apuane.  
726 *Bollettino del Regio Comitato Geologico d'Italia* 13, 82-91.

727 Ludwig, K.R., 2003. Isoplot 3.00: A geochronological toolkit for Microsoft Excel. Berkeley  
728 Geochronol. Center, Special Publication 4, 71 p.

729 Marroni, M., Tribuzio, R., 1996. Gabbro-derived granulites from External Liguride units (northern  
730 Apennine, Italy): Implications for the rifting processes in the western Tethys. *International*  
731 *Journal of Earth Sciences* 85, 239-249.

732 Marroni, M., Molli, G., Montanini, A., Tribuzio, R., 1998. The association of continental crust  
733 rocks with ophiolites in the Northern Apennines (Italy): Implications for the continent-ocean  
734 transition in the Western Tethys. *Tectonophysics* 292, 43-66.

735 McDonough, W.F., Sun, S.-S., 1995. Composition of the Earth. *Chemical Geology* 120, 223-253.

736 Meli, S., Montanini, A., Thöni, M., Frank, W., 1996. Age of mafic granulite blocks from the  
737 External Liguride Units (northern Apennine, Italy). *Memorie di Scienze Geologiche*  
738 *dell'Università di Padova* 48, 65-72.

739 Molli, G., 2008. Northern Apennine-Corsica orogenic system: an updated review. In: Siegesmund,  
740 S., Fügenschuh, B., Froitzheim, N. (Eds.), *Tectonic aspects of the Alpine-Dinaride-*  
741 *Carpathian System*. Geological Society of London, Special Publication 298, 413-442.

742 Molli, G., Montanini, A., Frank, W., 2002. MORB-derived Variscan amphibolites in the Northern  
 743 Apennine Basement: The Cerreto metamorphic slices (Tuscan-Emilian Apennine, NW Italy).  
 744 *Ofioliti* 27, 17-30.

745 Molli, G., Vaselli, L., 2006. Structures, interferences patterns, and strain regime during midcrustal  
 746 deformation in the Alpi Apuane (Northern Apennines, Italy). *Special Paper of the Geological*  
 747 *Society of America* 414, 79-93.

748 Montanini, A., Tribuzio, R., 2001. Gabbro-derived granulites from the Northern Apennines (Italy):  
 749 evidence for lower-crustal emplacement of tholeiitic liquids in post-Variscan times. *Journal of*  
 750 *Petrology* 42, 2259-2277.

751 Musumeci, G., Mazzarini, F., Tiepolo, M., Di Vincenzo, G., 2011. U-Pb and <sup>40</sup>Ar-<sup>39</sup>Ar  
 752 geochronology of Paleozoic units in the northern Apennines: determining protolith age and  
 753 alpine evolution using the Calamita Schist and Ortano Porphyroid. *Geological Journal* 46,  
 754 288-310.

755 Oggiano, G., Gaggero, L., Funedda, A., Buzzi, L., Tiepolo, M., 2010. Multiple early Paleozoic  
 756 volcanic events at the northern Gondwana margin: U-Pb age evidence from the southern  
 757 Variscan branch (Sardinia, Italy). *Gondwana Research* 17, 44-58.

758 Padovano, M., Elter, F.M., Pandeli, E., Franceschelli, M., 2012. The East Variscan Shear Zone: new  
 759 insights into its role in the Late Carboniferous collision in southern Europe. *International*  
 760 *Geology Review* 54, 957-970.

761 Pandeli, E., Gianelli, G., Puxeddu, M., Elter, F.M., 1994. The Paleozoic basement of the Northern  
 762 Apennines: stratigraphy, tectono-metamorphic evolution and Alpine hydrothermal processes.  
 763 *Memorie della Società Geologica Italiana* 48, 627-654.

764 Pandeli, E., Bagnoli, P., Negri, M., 2004. The Fornovolasco schists of the Apuan Alps (Northern  
 765 Tuscany, Italy): a new hypothesis for their stratigraphic setting. *Bollettino della Società*  
 766 *Geologica Italiana* 123, 53-66.

- 767 Paoli, G., Stokke, H.H., Rocchi, S., Sirevaag, H., Ksienzyk, A.K., Jacobs, J., Košler, J., 2017.  
768 Basement provenance revealed by U-Pb detrital zircon ages: A tale of African and European  
769 heritage in Tuscany, Italy. *Lithos* 277, 376-387.
- 770 Pearce, J.A., Harris, N.B.W., Tindle, A.G., 1984. Trace element discrimination diagrams for the  
771 tectonic interpretation of granitic rocks. *Journal of Petrology* 25, 956-983.
- 772 Perugini, D., Poli, G., 2007. Tourmaline nodules from Capo Bianco aplite (Elba Island, Italy): an  
773 example of diffusion limited aggregation growth in a magmatic system. *Contributions to*  
774 *Mineralogy and Petrology* 153, 493-508.
- 775 Petrelli, M., Morgavi, D., Vetere, F., Perugini, D., 2016. Elemental imaging and petro-  
776 volcanological applications of an improved Laser Ablation Inductively Coupled Quadrupole  
777 Plasma Mass Spectrometry. *Periodico di Mineralogia* 85, 25-39.
- 778 Petrus, J.A., Kamber, B.S., 2012. VizualAge: A novel approach to laser ablation ICP-MS U-Pb  
779 geochronology data reduction. *Geostandards and Geoanalytical Research* 36, 247-270.
- 780 Pieruccioni, D., Galanti, Y., Biagioni, C., Molli, G., 2018. The geological map of the Fornovolasco  
781 area, Apuan Alps (Tuscany, Italy). *Journal of Maps* 14, 357-367.
- 782 Plimer, I.R., Lees, T.C., 1988. Tourmaline-rich rocks associated with the submarine hydrothermal  
783 Rosebery Zn-Pb-Cu-Ag-Au deposit and granites in Western Tasmania, Australia. *Mineralogy*  
784 *and Petrology* 38, 81-103.
- 785 Pouchou, J.-L., Pichoir, F., 1991. Quantitative analysis of homogeneous or stratified microvolumes  
786 applying the model "PAP". In: Heinrich, K.F.J. and Newbury, D.E. (eds) *Electron Probe*  
787 *Quantification*. Plenum Press, New York, 31-75.
- 788 Prowatke, S., Ertl, A., Hughes, J.M., 2003. Tetrahedrally coordinated Al in Mn-rich, Li- and Fe-  
789 bearing olenite from Eibenstein an der Thaya, Lower Austria: A chemical and structural  
790 investigation. *Neues Jahrbuch für Mineralogie, Abhandlungen* 2003, 385-395.



791 Puxeddu, M., Saupé, F., Déchomets, R., Gianelli, G., Moine, B., 1984. Geochemistry and  
 792 stratigraphic correlations – application to the investigation of geothermal and mineral  
 793 resources of Tuscany, Italy. *Chemical Geology* 43, 77-113.

794 Rau, A., 1990. Evolution of the Tuscan domain between the Upper Carboniferous and the Middle  
 795 Triassic: a new hypothesis. *Bollettino della Società Geologica Italiana* 109, 231-238.

796 Rieder, M., Cavazzini, G., D'yakonov, Yu.S., Frank-Kamenetskii, V.A., Gottardi, G., Guggenheim,  
 797 S., Koval', P.V., Müller, G., Neiva, A.M.R., Radoslovich, E.W., Robert, J.-L., Sassi, F.P.,  
 798 Takeda, H., Weiss, Z., Wones, D.R., 1998. Nomenclature of the micas. *The Canadian*  
 799 *Mineralogist* 36, 905-912.

800 Romeo, I., Lunar, R., Capote, R., Quesada, C., Dunning, G.R., Piña, R., Ortega, L., 2006. U-Pb age  
 801 constraints on Variscan magmatism and Ni-Cu-PGE metallogeny in the Ossa-Morena Zone  
 802 (SW Iberia). *Journal of the Geological Society* 163, 837-846.

803 Schuster, R., Stüwe, K., 2008. Permian magmatic event in the Alps. *Geology* 36, 603-606.

804 Sirevaag, H., Jacobs, J., Ksienzyk, A.K., Rocchi, S., Paoli, G., Jørgensen, H., Košler, J., 2017. From  
 805 Gondwana to Europe: The journey of Elba Island (Italy) as recorded by U-Pb detrital zircon  
 806 ages of Paleozoic metasedimentary rocks. *Gondwana Research* 38, 273-288.

807 Slack, J.F., 1996. Tourmaline associations with hydrothermal ore deposits. *Reviews in Mineralogy*  
 808 *and Geochemistry* 33, 559-643.

809 Sláma, J., Košler, J., Condon, D.J., Crowley, J.L., Gerdes, A., Hanchar, J.M., Horstwood, M.S.A.,  
 810 Morris, G.A., Nasdala, L., Norberg, N., Schaltegger, U., Schoene, B., Tubrett, M.N.,  
 811 Whitehouse, M.J., 2008. Plešovice zircon – A new natural reference material for U-Pb and Hf  
 812 isotopic microanalysis. *Chemical Geology* 249, 1-35.

813 Stampfli, G.M., Borel, G.D., 2002. A plate tectonic model for the Paleozoic and Mesozoic  
 814 constrained by dynamic plate boundaries and restored synthetic oceanic isochrons. *Earth and*  
 815 *Planetary Science Letters* 196, 17-33.

816 Stampfli, G.M., von Raumer, J.F., Borel, G.D., 2002. Paleozoic evolution of pre-Variscan terranes:  
817 from Gondwana to the Variscan collision. Geological Society of America Special Paper 364,  
818 263-280.

819 Tischendorf, G., Förster, H.-J., Gottesmann, B., Rieder, M., 2007. True and brittle micas:  
820 composition and solid-solution series. Mineralogical Magazine 71, 285-320.

821 Torres-Ruiz, J., Pesquera, A., Gil-Crespo, P.P., Velilla, N., 2003. Origin and petrogenetic  
822 implications of tourmaline-rich rocks in the Sierra Nevada (Betic Cordillera, southeastern  
823 Spain). Chemical Geology 197, 55-86.

824 Vai, G.B., 1972. Evidence of Silurian in the Apuane Alps (Tuscany, Italy). Giornale di Geologia 38,  
825 349-372.

826 Vernon, R.H., 2004. A practical guide to Rock Microstructure. Cambridge University Press.

827 Visonà, D., Fioretti, A.M., Poli, M.E., Zanferrari, A., Fanning, M., 2007. U-Pb SHRIMP zircon  
828 dating of andesite from the Dolomite area (NE Italy): geochronological evidence for the early  
829 onset of Permian Volcanism in the eastern part of the southern Alps. Swiss Journal of  
830 Geosciences 100, 313-324.

831 von Raumer, J.F., Bussy, F., Schaltegger, U., Schultz, B., Stampfli, G.M., 2013. Pre-Mesozoic  
832 Alpine basements – Their place in the European Paleozoic framework. Geological Society of  
833 America Bulletin, 125, 89-108.

834 Wiewióra, A., Weiss, Z., 1990. Crystallochemical classifications of phyllosilicates based on the  
835 unified system of projection of chemical composition: II. The chlorite group. Clay Minerals  
836 25, 83-92.

837 Williams, M.L., Burr, J.L., 1994. Preservation and evolution of quartz phenocrysts in deformed  
838 rhyolites from the Proterozoic of southwestern North America. Journal of Structural Geology  
839 16, 203-221.

840 Winchester, J.A., Floyd, P.A., 1977. Geochemical discrimination of different magma series and  
841 their differentiation products using immobile elements. Chemical Geology 20, 325-343.

842 Zibra, I., Kruhl, J.H., Braga, R., 2010. Late Paleozoic deformation of post-Variscan lower crust:  
843 shear zone widening due to strain localization during retrograde shearing. International  
844 Journal of Earth Sciences, 99, 973-991.

845

846 **Table Captions**

847 **Table 1.** Details of the metarhyolite rock samples from Alpi Apuane studied in this work.

848 **Table 2.** Chemical analyses of phyllosilicates occurring in the Fornovolasco metarhyolite.

849 **Table 3.** Selected chemical analyses of tourmaline occurring in the Fornovolasco metarhyolite.

850 **Table 4.** Major- and trace-element analyses of metarhyolite rock samples from Alpi Apuane studied  
851 in this work.

852 **Table 5.** Summary of LA-ICP-MS U-Pb zircon datings of the Fornovolasco metarhyolite.

853

854 **Figure Captions**

855 **Fig. 1.** Geological sketch map of the Alpi Apuane Metamorphic Complex (based on Carmignani  
856 and Kligfield, 1990 and modified after Molli and Vaselli, 2006). The studied area is shown in the  
857 boxed frame. Red circles indicate the sampling sites of “*Porfiroidi*” (1 = PORF1; 2 = PORF2; 3 =  
858 PORF3 – see Table 1).

859 **Fig. 2.** Simplified geological map of the southern Alpi Apuane showing the location of the outcrops  
860 of the Fornovolasco Metarhyolite Fm (same labels as in Table 1) and the main ore deposits: 1)  
861 Fornovolasco; 2) La Tana; 3) Buca della Vena; 4) Canale della Radice; 5) Bottino; 6) Monte Rocca;  
862 7) Argentiera di Sant’Anna; 8) Monte Arsiccio; 9) Buca dell’Angina; 10) Pollone; 11) Levigliani.  
863 The outcrop close to Le Casette (boxed area) is shown in detail in Figure 5.

864 **Fig. 3.** Field features of the Fornovolasco Metarhyolite Fm. a) Hand specimen showing the  
865 occurrence of cm-size black tourmaline spots (base of the triangle = 12 cm). Boscaccio,  
866 Fornovolasco; b) the massive and granular nature of the metarhyolite cropping out at Le Casette,  
867 Fornovolasco (detail in Fig. 4d); c) massive and porphyritic metarhyolite, with tourmaline spots,  
868 cropping out at Trimpello, Fornovolasco (details in Fig. 4c and 6); d) tourmaline veins and spots in  
869 the metarhyolite body cropping out at Boscaccio, Fornovolasco; e) the black facies occurring at Le

870 Casette, Fornovolasco; f) Ti-rich pyrite veins embedded in the metarhyolite, with black tourmaline  
871 spots. Boscaccio, Fornovolasco.

872 **Fig. 4.** Polished slabs of specimens of the Fornovolasco Metarhyolite, showing some textural  
873 details. a) Foliated metarhyolite, with tourmaline spots wrapped by the main foliation. Boscaccio,  
874 Fornovolasco; b) porphyritic metarhyolite with quartz phenocrysts from Sant’Anna di Stazzema; c)  
875 porphyritic metarhyolite, with quartz and feldspar phenocrysts, from Trimpello, Fornovolasco; d)  
876 granular metarhyolite, with abundant black tourmaline, from Le Casette, Fornovolasco. Labels as in  
877 Table 1.

878 **Fig. 5.** (a) Geological map and cross-section showing the outcrops of the Fornovolasco  
879 Metarhyolite Fm at Le Casette, Fornovolasco. In the cross-section, the thin red lines indicate the  
880 relics of Variscan foliation. (b) Detail of the contact (red line) between the “*Filladi inferiori*” Fm  
881 (FAF), showing a pervasive foliation (light blue lines), and the massive rocks belonging to the  
882 Fornovolasco Metarhyolite Fm (FMR). Boscaccio, Fornovolasco.

883 **Fig. 6.** Petrographic features of the Fornovolasco Metarhyolite. a) Porphyritic texture, showing  
884 phenocrysts of quartz and sericitized feldspars. b) Quartz phenocrysts, with euhedral to subhedral  
885 morphology, in a sericitized groundmass. c) Tourmaline spot, formed by the intimate association of  
886 tourmaline + quartz, wrapped by the Alpine schistosity. d) Quartz phenocrysts with magmatic  
887 embayment, in a sericitized groundmass. e) Euhedral quartz phenocryst. f) Euhedral crystal of  
888 twinned feldspar, with an incipient crystallization of white mica. g) Biotite flakes, partially replaced  
889 by chlorite. h) Subhedral crystals of tourmaline showing a distinct zoning. Abbreviations: Bt,  
890 biotite; Chl, chlorite; Qz, quartz; Tur, tourmaline; Fld psd, feldspar pseudomorph.

891 **Fig. 7.** Chemical composition of tourmaline from the Fornovolasco metarhyolite plotted in the Al-  
892 Fe(tot)-Mg (a) and Ca-Fe(tot)-Mg (b) diagrams. Symbols: squares = FVb7; circles = FVb9; black  
893 crosses = tourmalinite (Benvenuti et al., 1991); black stars = “*Filladi inferiori*” Fm (Benvenuti et

894 al., 1991); and white stars = “*Porfiroidi e Scisti porfirici*” Fm (Benvenuti et al., 1991).  
 895 Compositional fields after Henry and Guidotti (1985). In (a): (1) Li-rich granitoid pegmatites and  
 896 aplites; (2) Li-poor granitoids and their associated pegmatites and aplites; (3) Fe<sup>3+</sup>-rich quartz-  
 897 tourmaline rocks (hydrothermally altered granites); (4) metapelites and metapsammites coexisting  
 898 with an Al-saturating phase; (5) metapelites and metapsammites not coexisting with an Al-  
 899 saturating phase; (6) Fe<sup>3+</sup>-rich quartz-tourmaline rocks, calc-silicate rocks, and metapelites; (7) low-  
 900 Ca metaultramafics and Cr,V-rich metasediments; (8) metacarbonates and meta-pyroxenites. In (b):  
 901 (1) Li-rich granitoid pegmatites and aplites; (2) Li-poor granitoids and associated pegmatites and  
 902 aplites; (3) Ca-rich metapelites, metapsammites, and calc-silicate rocks; (4) Ca-poor metapelites,  
 903 metapsammites, and quartz-tourmaline rocks; (5) metacarbonates; (6) metaultramafics.

904 **Fig. 8.** a) Total Alkali vs Silica classification diagram (Le Bas et al., 1986); b) Zr/TiO<sub>2</sub> vs Nb/Y  
 905 classification diagram (Winchester and Floyd, 1977).

906 **Fig. 9.** a) Incompatible element distribution of the studied felsic metavolcanic rocks. Element  
 907 concentrations are normalized to the Primitive Mantle composition of McDonough and Sun (1995).  
 908 b) REE distribution of the studied samples. Element concentrations are normalized to the CI  
 909 chondrite composition of McDonough and Sun (1995).

910 **Fig. 10.** Cathodoluminescence (SEM-CL) images of zircon crystals from the four selected samples.  
 911 Selected ages are shown.

912 **Fig. 11.** Histograms, probability density plot, and concordia diagram of LA-ICP-MS U-Pb zircon  
 913 ages of the Fornovolasco metarhyolite. The complete U-Pb data set is reported in Supplementary  
 914 Table S1.

915 **Fig. 12.** Histograms, probability density plots, and concordia diagrams of LA-ICP-MS U-Pb zircon  
 916 ages for the four samples of the Fornovolasco metarhyolite.

917 **Fig. 13.** Available geochronological data for the Paleozoic rocks cropping out in the Northern  
918 Apennines (in red). Ellipses report ages of magmatic rocks (red), of Variscan metamorphism  
919 (green), and the maximum depositional ages, based on detrital zircon (blue). References: (1) this  
920 work; (2) Eberhardt et al. (1962); (3) Lo Pò et al. (2016); (4) Molli et al. (2002); (5) Paoli et al.  
921 (2017); (6) Ferrara and Tonarini (1985); (7) Del Moro et al. (1982); (8) Sirevaag et al. (2016); (9)  
922 Musumeci et al. (2011).

923 **Table 1.** Details of the metarhyolite rock samples from Alpi Apuane studied in this work.

| <i>Sample</i>                      | <i>Locality</i>             | <i>UTM-E (m)*</i> | <i>UTM-N (m)*</i> | <i>Elevation<br/>(m a.m.s.l.)</i> | <i>Texture</i>          | <i>Mineralogy</i>         | <i>Tourmaline-bearing<br/>spots</i> |
|------------------------------------|-----------------------------|-------------------|-------------------|-----------------------------------|-------------------------|---------------------------|-------------------------------------|
| Fornovolasco Metarhyolite Fm       |                             |                   |                   |                                   |                         |                           |                                     |
| FVb1                               | Fornovolasco/Boscaccio      | 609552            | 4875911           | 475                               | Gra., unfoliated        | Qz, Wm, Tur               | No                                  |
| FVb2                               | Fornovolasco/Boscaccio      | 609830            | 4876168           | 610                               | Gra., slightly foliated | Qz, Fsp, Wm, Bt, Tur      | Common (< 1 cm)                     |
| FVb7                               | Fornovolasco/Boscaccio      | 609844            | 4876270           | 570                               | Por., unfoliated        | Qz, Fsp, Wm, Bt, Tur, Chl | Rare (< 1 cm)                       |
| FVb9                               | Fornovolasco/Boscaccio      | 609684            | 4876496           | 575                               | Por., slightly foliated | Qz, Wm, Bt, Tur, Chl      | Rare (< 5 mm)                       |
| FVb13                              | Fornovolasco/Boscaccio      | 609853            | 4876280           | 570                               | Por., unfoliated        | Qz, Fsp, Wm, Bt, Tur, Chl | Common (< 3 cm)                     |
| FVc1                               | Fornovolasco/Le Casette     | 608227            | 4875263           | 600                               | Gra., unfoliated        | Qz, Fsp, Wm, Tur          | No                                  |
| FVc2                               | Fornovolasco/Le Casette     | 608253            | 4875258           | 585                               | Gra., unfoliated        | Qz, Wm, Tur               | No                                  |
| FVc8                               | Fornovolasco/Le Casette     | 608253            | 4875259           | 585                               | Gra., unfoliated        | Qz, Fsp, Wm, Tur          | No                                  |
| FVt3                               | Fornovolasco/Trimpello      | 609198            | 4876438           | 675                               | Por., slightly foliated | Qz, Fsp, Wm, Tur, Chl     | Rare (< 2 cm)                       |
| POL1                               | Valdicastello Carducci      | 602240            | 4868881           | 290                               | Por., slightly foliated | Qz, Wm, Tur               | Common (< 2 cm)                     |
| MUL1                               | Mulina di Stazzema          | 604858            | 4870984           | 410                               | Por., unfoliated        | Qz, Fsp, Wm, Tur          | Rare (< 1 cm)                       |
| SAS1                               | Sant'Anna di Stazzema       | 602184            | 4869898           | 650                               | Por., slightly foliated | Qz, Fsp, Wm, Bt, Tur, Chl | Rare (< 2 cm)                       |
| "Porfiroidi e scisti porfirici" Fm |                             |                   |                   |                                   |                         |                           |                                     |
| PORF1                              | Passo del Pitone, Massa     | 597922            | 4878168           | 1220                              | Por., strongly foliated | Qz, Fsp, Wm               | No                                  |
| PORF2                              | Monte dei Ronchi, Seravezza | 600292            | 4878164           | 1275                              | Por., strongly foliated | Qz, Wm                    | No                                  |
| PORF3                              | Fociomboli, Stazzema        | 602613            | 4877421           | 1230                              | Por., strongly foliated | Qz, Wm                    | No                                  |

924 Abbreviations: Qz, quartz; Tur, tourmaline; Wm, white mica; Chl, chlorite; Bt, biotite; Fsp, feldspar. Gra., granular; Por., porphyritic; a.m.s.l., above mean sea level.

925 \*Coordinate system: WGS84-UTM32N

926



**Table 2.** Chemical analyses of phyllosilicates occurring in the Fornovolasco metarhyolite.

|                                    | biotite              |        | chlorite             |        | FVb7 dark (n = 7)    |        | FVb7 bright (n = 19) |        | muscovite            |        | FVb9 bright (n = 6)  |        | SAS1 (n = 8)         |        |
|------------------------------------|----------------------|--------|----------------------|--------|----------------------|--------|----------------------|--------|----------------------|--------|----------------------|--------|----------------------|--------|
|                                    | FVb7 (n = 28)        |        | SAS1 (n = 37)        |        |                      |        |                      |        | FVb9 dark (n = 12)   |        |                      |        |                      |        |
|                                    | wt%                  | e.s.d. | wt%                  | e.s.d. | wt%                  | e.s.d. | wt%                  | e.s.d. | wt%                  | e.s.d. | wt%                  | e.s.d. | wt%                  | e.s.d. |
| SiO <sub>2</sub>                   | 36.33                | 0.99   | 24.87                | 0.61   | 46.42                | 0.65   | 48.06                | 1.45   | 46.60                | 1.31   | 44.92                | 1.88   | 47.82                | 1.12   |
| TiO <sub>2</sub>                   | 2.70                 | 0.24   | 0.07                 | 0.04   | 0.05                 | 0.02   | 0.41                 | 0.16   | 0.39                 | 0.16   | 0.26                 | 0.12   | 0.28                 | 0.13   |
| Al <sub>2</sub> O <sub>3</sub>     | 13.95                | 0.44   | 20.34                | 0.64   | 34.71                | 1.20   | 24.19                | 0.86   | 30.91                | 1.92   | 30.21                | 1.30   | 27.48                | 1.13   |
| Cr <sub>2</sub> O <sub>3</sub>     | 0.04                 | 0.03   | -                    | -      | 0.02                 | 0.01   | -                    | -      | -                    | -      | -                    | -      | -                    | -      |
| V <sub>2</sub> O <sub>3</sub>      | 0.29                 | 0.04   | 0.03                 | 0.02   | -                    | -      | -                    | -      | -                    | -      | -                    | -      | 0.02                 | 0.01   |
| MgO                                | 8.56                 | 0.29   | 15.13                | 0.53   | 0.54                 | 0.25   | 3.26                 | 0.44   | 1.86                 | 0.68   | 1.18                 | 0.05   | 2.55                 | 0.36   |
| CaO                                | -                    | -      | 0.03                 | 0.02   | 0.03                 | 0.02   | -                    | -      | -                    | -      | -                    | -      | -                    | -      |
| MnO                                | 0.05                 | 0.03   | 0.18                 | 0.03   | 0.05                 | 0.04   | -                    | -      | -                    | -      | -                    | -      | -                    | -      |
| FeO                                | 23.26                | 0.49   | 24.49                | 0.63   | 1.24                 | 0.60   | 6.02                 | 1.45   | 2.16                 | 0.42   | 3.56                 | 0.31   | 2.96                 | 0.45   |
| SrO                                | -                    | -      | -                    | -      | -                    | -      | -                    | -      | -                    | -      | 0.07                 | 0.04   | -                    | -      |
| BaO                                | -                    | -      | -                    | -      | 0.08                 | 0.04   | 0.96                 | 0.41   | 0.08                 | 0.11   | 1.46                 | 0.07   | 0.14                 | 0.11   |
| Na <sub>2</sub> O                  | 0.03                 | 0.02   | -                    | -      | 0.11                 | 0.08   | 0.04                 | 0.02   | 0.19                 | 0.03   | 0.15                 | 0.02   | 0.23                 | 0.16   |
| K <sub>2</sub> O                   | 8.83                 | 0.34   | -                    | -      | 10.82                | 0.23   | 10.24                | 0.42   | 10.30                | 0.15   | 9.96                 | 0.14   | 10.60                | 0.18   |
| F                                  | 0.13                 | 0.03   | -                    | -      | -                    | -      | -                    | -      | -                    | -      | -                    | -      | -                    | -      |
| H <sub>2</sub> O <sub>calc</sub> * | 3.75                 |        | 11.05                |        | 4.45                 |        | 4.25                 |        | 4.36                 |        | 4.23                 |        | 4.30                 |        |
| O = F                              | -0.05                |        | -                    |        |                      |        |                      |        |                      |        |                      |        |                      |        |
| Total                              | 97.86                |        | 96.16                |        | 98.52                |        | 97.43                |        | 96.85                |        | 96.00                |        | 96.38                |        |
| apfu                               | normalized to O = 12 |        | normalized to O = 18 |        | normalized to O = 12 |        | normalized to O = 12 |        | normalized to O = 12 |        | normalized to O = 12 |        | normalized to O = 12 |        |
| Si <sup>4+</sup>                   | 2.86                 |        | 2.70                 |        | 3.13                 |        | 3.38                 |        | 3.21                 |        | 3.18                 |        | 3.33                 |        |
| <sup>IV</sup> Al <sup>3+</sup>     | 1.14                 |        | 1.30                 |        | 0.87                 |        | 0.62                 |        | 0.79                 |        | 0.82                 |        | 0.67                 |        |
| Ti <sup>4+</sup>                   | 0.16                 |        | 0.01                 |        | -                    |        | 0.02                 |        | 0.02                 |        | 0.01                 |        | 0.01                 |        |
| <sup>VI</sup> Al <sup>3+</sup>     | 0.15                 |        | 1.30                 |        | 1.89                 |        | 1.39                 |        | 1.72                 |        | 1.70                 |        | 1.59                 |        |
| Cr <sup>3+</sup>                   | -                    |        | -                    |        | -                    |        | -                    |        | -                    |        | -                    |        | -                    |        |
| V <sup>3+</sup>                    | 0.02                 |        | -                    |        | -                    |        | -                    |        | -                    |        | -                    |        | -                    |        |
| Mg <sup>2+</sup>                   | 1.00                 |        | 2.45                 |        | 0.05                 |        | 0.34                 |        | 0.19                 |        | 0.12                 |        | 0.26                 |        |
| Ca <sup>2+</sup>                   | -                    |        | -                    |        | -                    |        | -                    |        | -                    |        | -                    |        | -                    |        |
| Mn <sup>2+</sup>                   | -                    |        | 0.02                 |        | -                    |        | -                    |        | -                    |        | -                    |        | -                    |        |
| Fe <sup>2+</sup>                   | 1.53                 |        | 2.22                 |        | 0.07                 |        | 0.35                 |        | 0.12                 |        | 0.21                 |        | 0.17                 |        |
| Sr <sup>2+</sup>                   | -                    |        | -                    |        | -                    |        | -                    |        | -                    |        | -                    |        | -                    |        |
| Ba <sup>2+</sup>                   | -                    |        | -                    |        | -                    |        | 0.03                 |        | -                    |        | 0.04                 |        | -                    |        |
| Na <sup>+</sup>                    | -                    |        | -                    |        | 0.01                 |        | 0.01                 |        | 0.01                 |        | 0.02                 |        | 0.03                 |        |
| K <sup>+</sup>                     | 0.89                 |        | -                    |        | 0.93                 |        | 0.92                 |        | 0.90                 |        | 0.90                 |        | 0.94                 |        |
| F <sup>-</sup>                     | 0.03                 |        | -                    |        | -                    |        | -                    |        | -                    |        | -                    |        | -                    |        |
| OH <sup>-</sup>                    | 1.97                 |        | 8.00                 |        | 2.00                 |        | 2.00                 |        | 2.00                 |        | 2.00                 |        | 2.00                 |        |

\* H<sub>2</sub>O (wt%) calculated on the basis of stoichiometry. e.s.d., estimated standard deviation.

930  
931

**Table 3.** Selected chemical analyses of tourmaline occurring in the Fornovolasco metarhyolite.

|  | FVb7  |       |       |       |       | FVb9  |       |       |       |       |
|--|-------|-------|-------|-------|-------|-------|-------|-------|-------|-------|
|  | wt%   | wt%   | wt%   | wt%   | wt%   | wt%   | wt%   | wt%   | wt%   | wt%   |
| SiO <sub>2</sub>   | 35.41 | 33.62 | 36.23 | 35.51 | 35.89 | 36.05 | 37.99 | 37.38 | 34.29 | 35.93 |
| TiO <sub>2</sub>   | 4.22  | 0.10  | 0.25  | 4.62  | 0.05  | 0.04  | 0.27  | 0.11  | 1.32  | 1.76  |
| Al <sub>2</sub> O <sub>3</sub>   | 26.09 | 30.94 | 32.24 | 26.20 | 35.51 | 36.53 | 38.10 | 34.78 | 30.43 | 32.16 |
| V <sub>2</sub> O <sub>3</sub>  | 0.54  | -     | 0.05  | 0.51  | 0.04  | 0.02  | 0.05  | -     | 0.18  | 0.24  |
| MgO  | 6.10  | 4.94  | 5.68  | 6.32  | 2.82  | 2.93  | 8.62  | 8.03  | 6.75  | 6.88  |
| CaO  | 1.47  | 0.44  | 0.91  | 1.20  | 0.26  | 0.30  | 0.51  | 0.48  | 1.27  | 0.47  |
| MnO  | 0.07  | 0.06  | 0.16  | 0.07  | 0.05  | 0.06  | 0.01  | -     | 0.02  | -     |
| FeO  | 11.91 | 9.49  | 9.49  | 11.99 | 11.82 | 10.28 | 0.58  | 1.95  | 8.05  | 6.39  |
| SrO  | 0.15  | 0.06  | -     | 0.11  | -     | 0.04  | 0.23  | 0.04  | -     | -     |
| Na <sub>2</sub> O  | 2.19  | 2.00  | 2.13  | 2.36  | 1.85  | 1.75  | 2.24  | 2.54  | 1.92  | 2.16  |
| K <sub>2</sub> O   | 0.06  | 0.02  | 0.04  | 0.05  | 0.02  | 0.01  | 0.02  | 0.02  | 0.01  | 0.01  |
| Total  | 88.21 | 81.67 | 87.18 | 88.94 | 88.31 | 88.01 | 88.62 | 85.33 | 84.24 | 86.00 |
| apfu (normalized to O = 24.5, assuming 3 BO <sub>3</sub> groups and 4 OH groups) |       |       |       |       |       |       |       |       |       |       |
| T cations  |       |       |       |       |       |       |       |       |       |       |
| Si <sup>4+</sup>   | 5.91  | 5.89  | 5.94  | 5.88  | 5.83  | 5.82  | 5.82  | 5.98  | 5.81  | 5.87  |
| Al <sup>3+</sup>   | 0.09  | 0.11  | 0.06  | 0.12  | 0.17  | 0.18  | 0.18  | 0.02  | 0.19  | 0.13  |
| ΣT   | 6.00  | 6.00  | 6.00  | 6.00  | 6.00  | 6.00  | 6.00  | 6.00  | 6.00  | 6.00  |
| Z cations  |       |       |       |       |       |       |       |       |       |       |
| Al <sup>3+</sup>   | 5.04  | 6.00  | 6.00  | 4.99  | 6.00  | 6.00  | 6.00  | 6.00  | 5.89  | 6.00  |
| Mg <sup>2+</sup>   | 0.96  | -     | -     | 1.11  | -     | -     | -     | -     | 0.11  | -     |
| ΣT   | 6.00  | 6.00  | 6.00  | 6.00  | 6.00  | 6.00  | 6.00  | 6.00  | 6.00  | 6.00  |
| Y cations  |       |       |       |       |       |       |       |       |       |       |
| Ti <sup>4+</sup>   | 0.53  | 0.01  | 0.03  | 0.57  | 0.01  | -     | 0.03  | 0.01  | 0.17  | 0.22  |
| Al <sup>3+</sup>   | -     | 0.28  | 0.17  | -     | 0.63  | 0.77  | 0.70  | 0.54  | -     | 0.07  |
| V <sup>3+</sup>  | 0.07  | -     | 0.01  | 0.07  | 0.01  | -     | 0.01  | -     | 0.02  | 0.03  |
| Mg <sup>2+</sup>   | 0.56  | 1.29  | 1.39  | 0.45  | 0.68  | 0.70  | 1.97  | 1.92  | 1.59  | 1.68  |
| Mn <sup>2+</sup>   | 0.01  | 0.01  | 0.02  | 0.01  | 0.01  | 0.01  | -     | -     | -     | -     |
| Fe <sup>2+</sup>   | 1.66  | 1.39  | 1.30  | 1.66  | 1.60  | 1.39  | 0.07  | 0.26  | 1.14  | 0.87  |
| ΣY   | 2.83  | 2.98  | 2.92  | 2.76  | 2.94  | 2.87  | 2.71  | 2.73  | 2.92  | 2.87  |
| X cations  |       |       |       |       |       |       |       |       |       |       |
| Ca <sup>2+</sup>   | 0.26  | 0.08  | 0.16  | 0.21  | 0.05  | 0.05  | 0.08  | 0.08  | 0.23  | 0.08  |
| Sr <sup>2+</sup>   | 0.01  | 0.01  | -     | 0.01  | -     | -     | 0.02  | -     | -     | -     |
| Na <sup>+</sup>  | 0.71  | 0.68  | 0.68  | 0.76  | 0.58  | 0.55  | 0.67  | 0.79  | 0.63  | 0.68  |
| K <sup>+</sup>   | 0.01  | -     | 0.01  | 0.01  | -     | -     | -     | -     | -     | -     |
| ΣX   | 0.99  | 0.77  | 0.85  | 0.99  | 0.63  | 0.60  | 0.77  | 0.87  | 0.86  | 0.76  |

932

933 **Table 4.** Major- and trace-element analyses of metarhyolite rock samples from Alpi  
934 Apuane studied in this work.

| Sample                             | <i>Fornovolasco Metarhyolite Fm</i> |       |       |       |       |        | <i>"Porfiroidi e scisti porfirici" Fm</i> |        |       |       |
|------------------------------------|-------------------------------------|-------|-------|-------|-------|--------|---|--------|-------|-------|
|                                    | FVb1                                | FVb2  | FVb13 | FVc2  | FVc8  | SAS1   | MUL1                                      | PORF1  | PORF2 | PORF3 |
| <i>Major elements (wt%)</i>        |                                     |       |       |       |       |        |   |        |       |       |
| SiO <sub>2</sub>                   | 73.18                               | 74.73 | 69.19 | 73.68 | 74.34 | 69.66  | 75.23                                     | 67.39  | 76.42 | 70.28 |
| TiO <sub>2</sub>                   | 0.24                                | 0.23  | 0.44  | 0.26  | 0.26  | 0.43   | 0.39                                      | 0.78   | 0.38  | 0.43  |
| Al <sub>2</sub> O <sub>3</sub>     | 13.60                               | 14.07 | 15.14 | 14.54 | 14.52 | 14.98  | 14.41                                     | 15.32  | 13.39 | 14.19 |
| Fe <sub>2</sub> O <sub>3 tot</sub> | 2.89                                | 1.74  | 3.30  | 1.80  | 2.02  | 2.94   | 1.20                                      | 5.52   | 1.60  | 3.24  |
| MnO                                | 0.01                                | 0.03  | 0.10  | 0.02  | 0.07  | 0.06   | 0.01                                      | 0.06   | 0.01  | 0.06  |
| MgO                                | 0.93                                | 0.72  | 1.46  | 1.31  | 0.67  | 1.71   | 0.50                                      | 1.47   | 0.69  | 0.65  |
| CaO                                | 0.17                                | 0.20  | 0.73  | 0.32  | 0.19  | 1.11   | 0.17                                      | 0.23   | 0.08  | 0.82  |
| Na <sub>2</sub> O                  | 0.29                                | 3.92  | 1.81  | 0.27  | 1.14  | 3.84   | 2.85                                      | 2.98   | 0.14  | 2.59  |
| K <sub>2</sub> O                   | 3.30                                | 2.38  | 4.54  | 4.57  | 3.74  | 2.68   | 3.03                                      | 3.38   | 4.42  | 4.95  |
| P <sub>2</sub> O <sub>5</sub>      | 0.13                                | 0.14  | 0.23  | 0.13  | 0.14  | 0.16   | 0.12                                      | 0.23   | 0.13  | 0.19  |
| LOI                                | 2.85                                | 1.45  | 2.33  | 2.49  | 1.75  | 2.48   | 1.86                                      | 2.64   | 2.18  | 2.18  |
| Total                              | 97.59                               | 99.61 | 99.27 | 99.39 | 98.84 | 100.05 | 99.77                                     | 100.00 | 99.44 | 99.58 |
| <i>Trace elements (ppm)</i>        |                                     |       |       |       |       |        |   |        |       |       |
| Be                                 | 4                                   | 3     | 4     | 4     | 4     | 3      | 2   | 3      | 3     | 2     |
| Sc                                 | 6                                   | 4     | 7     | 4     | 4     | 8      | 6   | 13     | 7     | 7     |
| V                                  | 23                                  | 21    | 47    | 28    | 27    | 49     | 43  | 74     | 26    | 34    |
| Cr                                 | < 20                                | < 20  | 50    | < 20  | 30    | 30     | 30  | 50     | < 20  | 30    |
| Co                                 | < 1                                 | 2     | 11    | < 1   | 4     | 5      | 2   | 12     | 1     | 8     |
| Ni                                 | < 20                                | < 20  | 30    | < 20  | < 20  | 20     | < 20                                      | 20     | < 20  | < 20  |
| Cu                                 | 260                                 | < 10  | 30    | < 10  | < 10  | < 10   | 40  | 20     | < 10  | 20    |
| Ga                                 | 17                                  | 14    | 17    | 18    | 18    | 16     | 15  | 20     | 17    | 18    |
| Ge                                 | 2.3                                 | 2.2   | 2.4   | 2.3   | 1.9   | 1.9    | 1.8                                       | 1.1    | 1.2   | 1.1   |
| As                                 | > 2000                              | 326   | 1120  | 75    | 58    | < 5    | 191                                       | 10     | 24    | 12    |
| Rb                                 | 116                                 | 99    | 214   | 176   | 124   | 86     | 110                                       | 112    | 138   | 111   |
| Sr                                 | 17                                  | 99    | 69    | 15    | 18    | 106    | 48  | 46     | 18    | 35    |
| Y                                  | 10.9                                | 8.4   | 18.2  | 12.3  | 11.5  | 16.6   | 16.4                                      | 40.9   | 36.6  | 35    |
| Zr                                 | 91                                  | 76    | 130   | 108   | 93    | 146    | 133                                       | 321    | 256   | 208   |
| Nb                                 | 7.1                                 | 7.0   | 7.5   | 8.0   | 7.1   | 7.8    | 6.1                                       | 14.9   | 11.1  | 11.6  |
| Ag                                 | 1.4                                 | < 0.5 | 0.6   | 0.6   | < 0.5 | 0.6    | 1.0                                       | 1.3    | 1.0   | 0.9   |
| Sn                                 | 24                                  | 10    | 10    | 17    | 17    | 3      | 5   | 3      | 3     | 4     |
| Sb                                 | > 200                               | 5.4   | 21.1  | 6.7   | 3.9   | 1.3    | 6.9                                       | 1.6    | 5.7   | 1.5   |
| Cs                                 | 5.7                                 | 8.6   | 21.9  | 5.8   | 3.9   | 3.3    | 6.1                                       | 5.1    | 8.4   | 6.0   |
| Ba                                 | 377                                 | 933   | 654   | 155   | 139   | 400    | 384                                       | 684    | 807   | 935   |
| Hf                                 | 2.4                                 | 2.1   | 3.3   | 2.8   | 2.6   | 3.7    | 3.5                                       | 8.1    | 6.1   | 5.4   |
| Ta                                 | 1.02                                | 1.46  | 0.98  | 1.14  | 1.13  | 1.03   | 0.94                                      | 1.03   | 0.92  | 0.95  |
| W                                  | 2.0                                 | 1.7   | 6.5   | 2.0   | 1.4   | 2.1    | 5.9                                       | 1.7    | 1.7   | 1.6   |
| Tl                                 | 2.68                                | 3.84  | 10.4  | 4.19  | 3.58  | 1.21   | 3.57                                      | 1.09   | 1.02  | 0.75  |
| Pb                                 | 1060                                | 48    | 256   | 22    | 13    | 6      | 157                                       | 21     | 27    | 12    |
| Bi                                 | 58.1                                | 3.3   | 50.8  | 38.9  | 1.6   | < 0.1  | 2.1                                       | 0.8    | 0.3   | 0.1   |
| Th                                 | 9.20                                | 5.52  | 9.58  | 10.1  | 9.36  | 10.2   | 9.19                                      | 19.3   | 18.3  | 15.9  |
| U                                  | 3.18                                | 2.69  | 4.44  | 1.82  | 1.72  | 2.05   | 2.11                                      | 3.03   | 2.94  | 4.13  |
| La                                 | 26.9                                | 16.5  | 24.5  | 37.7  | 24.7  | 21.1   | 26.1                                      | 55.5   | 62    | 47.1  |
| Ce                                 | 54.4                                | 34.8  | 50.8  | 76.5  | 48.2  | 42.3   | 49.0                                      | 118    | 125   | 95.4  |
| Pr                                 | 5.93                                | 3.91  | 5.70  | 8.51  | 5.56  | 4.9    | 5.98                                      | 13.3   | 13.9  | 10.9  |
| Nd                                 | 21.1                                | 14.0  | 20.6  | 31.0  | 20.6  | 17.9   | 22.5                                      | 50.4   | 51.1  | 40.7  |
| Sm                                 | 4.48                                | 2.97  | 4.56  | 6.47  | 4.34  | 3.97   | 4.58                                      | 10.4   | 9.78  | 8.50  |
| Eu                                 | 0.64                                | 0.692 | 0.966 | 0.949 | 0.621 | 1.04   | 0.741                                     | 1.38   | 1.23  | 1.23  |
| Gd                                 | 2.69                                | 2.28  | 3.93  | 4.48  | 3.05  | 3.48   | 3.79                                      | 9.01   | 7.84  | 7.55  |
| Tb                                 | 0.37                                | 0.33  | 0.56  | 0.57  | 0.43  | 0.55   | 0.60                                      | 1.35   | 1.11  | 1.18  |
| Dy                                 | 1.88                                | 1.73  | 3.12  | 2.58  | 2.12  | 3.12   | 3.25                                      | 7.58   | 6.30  | 6.64  |
| Ho                                 | 0.34                                | 0.30  | 0.56  | 0.41  | 0.37  | 0.58   | 0.6                                       | 1.44   | 1.2   | 1.23  |
| Er                                 | 0.99                                | 0.81  | 1.60  | 1.06  | 1.05  | 1.55   | 1.75                                      | 4.03   | 3.45  | 3.39  |
| Tm                                 | 0.155                               | 0.119 | 0.214 | 0.134 | 0.147 | 0.227  | 0.235                                     | 0.585  | 0.504 | 0.455 |
| Yb                                 | 1.04                                | 0.77  | 1.38  | 0.83  | 0.99  | 1.60   | 1.57                                      | 3.89   | 3.32  | 2.93  |
| Lu                                 | 0.166                               | 0.123 | 0.228 | 0.131 | 0.152 | 0.234  | 0.248                                     | 0.560  | 0.496 | 0.475 |

935  
936

937 **Table 5.** Summary of LA-ICP-MS U-Pb zircon datings of the Fornovolasco metarhyolite.

| Sample | Zircon crystals<br>imaged by<br>SEM-CL | Zircon crystals<br>selected for U-Pb<br>dating | LA<br>spots | Number of U-<br>Pb concordant<br>ages* | Age (Ma)                              |                       |                       |
|--------|--|--|-------------|--|---------------------------------------|-----------------------|-----------------------|
|        |  |  |             |  | weighted<br>average ( $\pm 2\sigma$ ) | min ( $\pm 2\sigma$ ) | max ( $\pm 2\sigma$ ) |
| FVb13  | 116                                    | 82   | 122         | rims                                   | 36                                    | 271.0 ( $\pm 3.5$ )   | 241.8 ( $\pm 4.0$ )   |
|        |  |  |             | cores                                  | 10                                    | 276.8 ( $\pm 8.8$ )   | 260.3 ( $\pm 7.2$ )   |
| FVc1   | 80                                     | 61   | 85          | rims                                   | 40                                    | 279.7 ( $\pm 3.4$ )   | 256.0 ( $\pm 6.2$ )   |
|        |  |  |             | cores                                  | 7                                     | 282.6 ( $\pm 6.6$ )   | 270.0 ( $\pm 5.6$ )   |
| POL1   | 107                                    | 55   | 73          | rims                                   | 24                                    | 276.7 ( $\pm 8.5$ )   | 226.5 ( $\pm 6.3$ )   |
|        |  |  |             | cores                                  | 0                                     | -                     | -                     |
| SAS1   | 114                                    | 80   | 106         | rims                                   | 44                                    | 291.8 ( $\pm 3.2$ )   | 258.6 ( $\pm 6.6$ )   |
|        |  |  |             | cores                                  | 8                                     | 290.2 ( $\pm 6.2$ )   | 280.7 ( $\pm 4.8$ )   |
|        |  |  |             | All                                    | 169                                   | 279.9 ( $\pm 2.0$ )   | 310.6 ( $\pm 5.4$ )   |

938 \*The cutoff limit was set to 3% normal discordance  $\{[(^{206}\text{Pb}/^{238}\text{U age})/(^{207}\text{Pb}/^{235}\text{U age}) - 1]*100\}$ .

939

917 **Fig. 13.** Available geochronological data for the Paleozoic rocks cropping out in the Northern  
918 Apennines (in red). Ellipses report ages of magmatic rocks (red), of Variscan metamorphism  
919 (green), and the maximum depositional ages, based on detrital zircon (blue). References: (1) this  
920 work; (2) Eberhardt et al. (1962); (3) Lo Pò et al. (2016); (4) Molli et al. (2002); (5) Paoli et al.  
921 (2017); (6) Ferrara and Tonarini (1985); (7) Del Moro et al. (1982); (8) Sirevaag et al. (2016); (9)  
922 Musumeci et al. (2011).

923 **Table 1.** Details of the metarhyolite rock samples from Alpi Apuane studied in this work.

| Sample                             | Locality                    | UTM-E (m)* | UTM-N (m)* | Elevation<br>(m a.m.s.l.) | Texture                 | Mineralogy                | Tourmaline-bearing<br>spots |
|------------------------------------|-----------------------------|------------|------------|---------------------------|-------------------------|---------------------------|-----------------------------|
| Fornovolasco Metarhyolite Fm       |                             |            |            |                           |                         |                           |                             |
| FVb1                               | Fornovolasco/Boscaccio      | 609552     | 4875911    | 475                       | Gra., unfoliated        | Qz, Wm, Tur               | No                          |
| FVb2                               | Fornovolasco/Boscaccio      | 609830     | 4876168    | 610                       | Gra., slightly foliated | Qz, Fsp, Wm, Bt, Tur      | Common (< 1 cm)             |
| FVb7                               | Fornovolasco/Boscaccio      | 609844     | 4876270    | 570                       | Por., unfoliated        | Qz, Fsp, Wm, Bt, Tur, Chl | Rare (< 1 cm)               |
| FVb9                               | Fornovolasco/Boscaccio      | 609684     | 4876496    | 575                       | Por., slightly foliated | Qz, Wm, Bt, Tur, Chl      | Rare (< 5 mm)               |
| FVb13                              | Fornovolasco/Boscaccio      | 609853     | 4876280    | 570                       | Por., unfoliated        | Qz, Fsp, Wm, Bt, Tur, Chl | Common (< 3 cm)             |
| FVc1                               | Fornovolasco/Le Casette     | 608227     | 4875263    | 600                       | Gra., unfoliated        | Qz, Fsp, Wm, Tur          | No                          |
| FVc2                               | Fornovolasco/Le Casette     | 608253     | 4875258    | 585                       | Gra., unfoliated        | Qz, Wm, Tur               | No                          |
| FVc8                               | Fornovolasco/Le Casette     | 608253     | 4875259    | 585                       | Gra., unfoliated        | Qz, Fsp, Wm, Tur          | No                          |
| FVt3                               | Fornovolasco/Trimpello      | 609198     | 4876438    | 675                       | Por., slightly foliated | Qz, Fsp, Wm, Tur, Chl     | Rare (< 2 cm)               |
| POL1                               | Valdicastello Carducci      | 602240     | 4868881    | 290                       | Por., slightly foliated | Qz, Wm, Tur               | Common (< 2 cm)             |
| MUL1                               | Mulina di Stazzema          | 604858     | 4870984    | 410                       | Por., unfoliated        | Qz, Fsp, Wm, Tur          | Rare (< 1 cm)               |
| SAS1                               | Sant'Anna di Stazzema       | 602184     | 4869898    | 650                       | Por., slightly foliated | Qz, Fsp, Wm, Bt, Tur, Chl | Rare (< 2 cm)               |
| "Porfiroidi e scisti porfirici" Fm |                             |            |            |                           |                         |                           |                             |
| PORF1                              | Passo del Pitone, Massa     | 597922     | 4878168    | 1220                      | Por., strongly foliated | Qz, Fsp, Wm               | No                          |
| PORF2                              | Monte dei Ronchi, Seravezza | 600292     | 4878164    | 1275                      | Por., strongly foliated | Qz, Wm                    | No                          |
| PORF3                              | Fociomboli, Stazzema        | 602613     | 4877421    | 1230                      | Por., strongly foliated | Qz, Wm                    | No                          |

924 Abbreviations: Qz, quartz; Tur, tourmaline; Wm, white mica; Chl, chlorite; Bt, biotite; Fsp, feldspar. Gra., granular; Por., porphyritic; a.m.s.l., above mean sea level.

925 \*Coordinate system: WGS84-UTM32N

926

**Table 2.** Chemical analyses of phyllosilicates occurring in the Fornovolasco metarhyolite.

|                                    | biotite              |        | chlorite             |        | muscovite            |        |                      |        |                      |        |                      |        |                      |        |
|------------------------------------|----------------------|--------|----------------------|--------|----------------------|--------|----------------------|--------|----------------------|--------|----------------------|--------|----------------------|--------|
|                                    | FVb7 (n = 28)        |        | SAS1 (n = 37)        |        | FVb7 dark (n = 7)    |        | FVb7 bright (n = 19) |        | FVb9 dark (n = 12)   |        | FVb9 bright (n = 6)  |        | SAS1 (n = 8)         |        |
|                                    | wt%                  | e.s.d. | wt%                  | e.s.d. | wt%                  | e.s.d. | wt%                  | e.s.d. | wt%                  | e.s.d. | wt%                  | e.s.d. | wt%                  | e.s.d. |
| SiO <sub>2</sub>                   | 36.33                | 0.99   | 24.87                | 0.61   | 46.42                | 0.65   | 48.06                | 1.45   | 46.60                | 1.31   | 44.92                | 1.88   | 47.82                | 1.12   |
| TiO <sub>2</sub>                   | 2.70                 | 0.24   | 0.07                 | 0.04   | 0.05                 | 0.02   | 0.41                 | 0.16   | 0.39                 | 0.16   | 0.26                 | 0.12   | 0.28                 | 0.13   |
| Al <sub>2</sub> O <sub>3</sub>     | 13.95                | 0.44   | 20.34                | 0.64   | 34.71                | 1.20   | 24.19                | 0.86   | 30.91                | 1.92   | 30.21                | 1.30   | 27.48                | 1.13   |
| Cr <sub>2</sub> O <sub>3</sub>     | 0.04                 | 0.03   | -                    | -      | 0.02                 | 0.01   | -                    | -      | -                    | -      | -                    | -      | -                    | -      |
| V <sub>2</sub> O <sub>3</sub>      | 0.29                 | 0.04   | 0.03                 | 0.02   | -                    | -      | -                    | -      | -                    | -      | -                    | -      | 0.02                 | 0.01   |
| MgO                                | 8.56                 | 0.29   | 15.13                | 0.53   | 0.54                 | 0.25   | 3.26                 | 0.44   | 1.86                 | 0.68   | 1.18                 | 0.05   | 2.55                 | 0.36   |
| CaO                                | -                    | -      | 0.03                 | 0.02   | 0.03                 | 0.02   | -                    | -      | -                    | -      | -                    | -      | -                    | -      |
| MnO                                | 0.05                 | 0.03   | 0.18                 | 0.03   | 0.05                 | 0.04   | -                    | -      | -                    | -      | -                    | -      | -                    | -      |
| FeO                                | 23.26                | 0.49   | 24.49                | 0.63   | 1.24                 | 0.60   | 6.02                 | 1.45   | 2.16                 | 0.42   | 3.56                 | 0.31   | 2.96                 | 0.45   |
| SrO                                | -                    | -      | -                    | -      | -                    | -      | -                    | -      | -                    | -      | 0.07                 | 0.04   | -                    | -      |
| BaO                                | -                    | -      | -                    | -      | 0.08                 | 0.04   | 0.96                 | 0.41   | 0.08                 | 0.11   | 1.46                 | 0.07   | 0.14                 | 0.11   |
| Na <sub>2</sub> O                  | 0.03                 | 0.02   | -                    | -      | 0.11                 | 0.08   | 0.04                 | 0.02   | 0.19                 | 0.03   | 0.15                 | 0.02   | 0.23                 | 0.16   |
| K <sub>2</sub> O                   | 8.83                 | 0.34   | -                    | -      | 10.82                | 0.23   | 10.24                | 0.42   | 10.30                | 0.15   | 9.96                 | 0.14   | 10.60                | 0.18   |
| F                                  | 0.13                 | 0.03   | -                    | -      | -                    | -      | -                    | -      | -                    | -      | -                    | -      | -                    | -      |
| H <sub>2</sub> O <sub>calc</sub> * | 3.75                 |        | 11.05                |        | 4.45                 |        | 4.25                 |        | 4.36                 |        | 4.23                 |        | 4.30                 |        |
| O = F                              | -0.05                |        | -                    |        |                      |        |                      |        |                      |        |                      |        |                      |        |
| Total                              | 97.86                |        | 96.16                |        | 98.52                |        | 97.43                |        | 96.85                |        | 96.00                |        | 96.38                |        |
| apfu                               | normalized to O = 12 |        | normalized to O = 18 |        | normalized to O = 12 |        | normalized to O = 12 |        | normalized to O = 12 |        | normalized to O = 12 |        | normalized to O = 12 |        |
| Si <sup>4+</sup>                   | 2.86                 |        | 2.70                 |        | 3.13                 |        | 3.38                 |        | 3.21                 |        | 3.18                 |        | 3.33                 |        |
| <sup>IV</sup> Al <sup>3+</sup>     | 1.14                 |        | 1.30                 |        | 0.87                 |        | 0.62                 |        | 0.79                 |        | 0.82                 |        | 0.67                 |        |
| Ti <sup>4+</sup>                   | 0.16                 |        | 0.01                 |        | -                    |        | 0.02                 |        | 0.02                 |        | 0.01                 |        | 0.01                 |        |
| <sup>VI</sup> Al <sup>3+</sup>     | 0.15                 |        | 1.30                 |        | 1.89                 |        | 1.39                 |        | 1.72                 |        | 1.70                 |        | 1.59                 |        |
| Cr <sup>3+</sup>                   | -                    |        | -                    |        | -                    |        | -                    |        | -                    |        | -                    |        | -                    |        |
| V <sup>3+</sup>                    | 0.02                 |        | -                    |        | -                    |        | -                    |        | -                    |        | -                    |        | -                    |        |
| Mg <sup>2+</sup>                   | 1.00                 |        | 2.45                 |        | 0.05                 |        | 0.34                 |        | 0.19                 |        | 0.12                 |        | 0.26                 |        |
| Ca <sup>2+</sup>                   | -                    |        | -                    |        | -                    |        | -                    |        | -                    |        | -                    |        | -                    |        |
| Mn <sup>2+</sup>                   | -                    |        | 0.02                 |        | -                    |        | -                    |        | -                    |        | -                    |        | -                    |        |
| Fe <sup>2+</sup>                   | 1.53                 |        | 2.22                 |        | 0.07                 |        | 0.35                 |        | 0.12                 |        | 0.21                 |        | 0.17                 |        |
| Sr <sup>2+</sup>                   | -                    |        | -                    |        | -                    |        | -                    |        | -                    |        | -                    |        | -                    |        |
| Ba <sup>2+</sup>                   | -                    |        | -                    |        | -                    |        | 0.03                 |        | -                    |        | 0.04                 |        | -                    |        |
| Na <sup>+</sup>                    | -                    |        | -                    |        | 0.01                 |        | 0.01                 |        | 0.01                 |        | 0.02                 |        | 0.03                 |        |
| K <sup>+</sup>                     | 0.89                 |        | -                    |        | 0.93                 |        | 0.92                 |        | 0.90                 |        | 0.90                 |        | 0.94                 |        |
| F <sup>-</sup>                     | 0.03                 |        | -                    |        | -                    |        | -                    |        | -                    |        | -                    |        | -                    |        |
| OH <sup>-</sup>                    | 1.97                 |        | 8.00                 |        | 2.00                 |        | 2.00                 |        | 2.00                 |        | 2.00                 |        | 2.00                 |        |

\* H<sub>2</sub>O (wt%) calculated on the basis of stoichiometry. e.s.d., estimated standard deviation.

930  
931

**Table 3.** Selected chemical analyses of tourmaline occurring in the Fornovolasco metarhyolite.

|  | FVb7  |       |       |       | FVb9  |       |       |       |       |       |
|--|-------|-------|-------|-------|-------|-------|-------|-------|-------|-------|
|  | wt%   | wt%   | wt%   | wt%   | wt%   | wt%   | wt%   | wt%   | wt%   | wt%   |
| SiO <sub>2</sub>   | 35.41 | 33.62 | 36.23 | 35.51 | 35.89 | 36.05 | 37.99 | 37.38 | 34.29 | 35.93 |
| TiO <sub>2</sub>   | 4.22  | 0.10  | 0.25  | 4.62  | 0.05  | 0.04  | 0.27  | 0.11  | 1.32  | 1.76  |
| Al <sub>2</sub> O <sub>3</sub>   | 26.09 | 30.94 | 32.24 | 26.20 | 35.51 | 36.53 | 38.10 | 34.78 | 30.43 | 32.16 |
| V <sub>2</sub> O <sub>3</sub>  | 0.54  | -     | 0.05  | 0.51  | 0.04  | 0.02  | 0.05  | -     | 0.18  | 0.24  |
| MgO  | 6.10  | 4.94  | 5.68  | 6.32  | 2.82  | 2.93  | 8.62  | 8.03  | 6.75  | 6.88  |
| CaO  | 1.47  | 0.44  | 0.91  | 1.20  | 0.26  | 0.30  | 0.51  | 0.48  | 1.27  | 0.47  |
| MnO  | 0.07  | 0.06  | 0.16  | 0.07  | 0.05  | 0.06  | 0.01  | -     | 0.02  | -     |
| FeO  | 11.91 | 9.49  | 9.49  | 11.99 | 11.82 | 10.28 | 0.58  | 1.95  | 8.05  | 6.39  |
| SrO  | 0.15  | 0.06  | -     | 0.11  | -     | 0.04  | 0.23  | 0.04  | -     | -     |
| Na <sub>2</sub> O  | 2.19  | 2.00  | 2.13  | 2.36  | 1.85  | 1.75  | 2.24  | 2.54  | 1.92  | 2.16  |
| K <sub>2</sub> O   | 0.06  | 0.02  | 0.04  | 0.05  | 0.02  | 0.01  | 0.02  | 0.02  | 0.01  | 0.01  |
| Total  | 88.21 | 81.67 | 87.18 | 88.94 | 88.31 | 88.01 | 88.62 | 85.33 | 84.24 | 86.00 |
| apfu (normalized to O = 24.5, assuming 3 BO <sub>3</sub> groups and 4 OH groups) |       |       |       |       |       |       |       |       |       |       |
| T cations  |       |       |       |       |       |       |       |       |       |       |
| Si <sup>4+</sup>   | 5.91  | 5.89  | 5.94  | 5.88  | 5.83  | 5.82  | 5.82  | 5.98  | 5.81  | 5.87  |
| Al <sup>3+</sup>   | 0.09  | 0.11  | 0.06  | 0.12  | 0.17  | 0.18  | 0.18  | 0.02  | 0.19  | 0.13  |
| ΣT   | 6.00  | 6.00  | 6.00  | 6.00  | 6.00  | 6.00  | 6.00  | 6.00  | 6.00  | 6.00  |
| Z cations  |       |       |       |       |       |       |       |       |       |       |
| Al <sup>3+</sup>   | 5.04  | 6.00  | 6.00  | 4.99  | 6.00  | 6.00  | 6.00  | 6.00  | 5.89  | 6.00  |
| Mg <sup>2+</sup>   | 0.96  | -     | -     | 1.11  | -     | -     | -     | -     | 0.11  | -     |
| ΣT   | 6.00  | 6.00  | 6.00  | 6.00  | 6.00  | 6.00  | 6.00  | 6.00  | 6.00  | 6.00  |
| Y cations  |       |       |       |       |       |       |       |       |       |       |
| Ti <sup>4+</sup>   | 0.53  | 0.01  | 0.03  | 0.57  | 0.01  | -     | 0.03  | 0.01  | 0.17  | 0.22  |
| Al <sup>3+</sup>   | -     | 0.28  | 0.17  | -     | 0.63  | 0.77  | 0.70  | 0.54  | -     | 0.07  |
| V <sup>3+</sup>  | 0.07  | -     | 0.01  | 0.07  | 0.01  | -     | 0.01  | -     | 0.02  | 0.03  |
| Mg <sup>2+</sup>   | 0.56  | 1.29  | 1.39  | 0.45  | 0.68  | 0.70  | 1.97  | 1.92  | 1.59  | 1.68  |
| Mn <sup>2+</sup>   | 0.01  | 0.01  | 0.02  | 0.01  | 0.01  | 0.01  | -     | -     | -     | -     |
| Fe <sup>2+</sup>   | 1.66  | 1.39  | 1.30  | 1.66  | 1.60  | 1.39  | 0.07  | 0.26  | 1.14  | 0.87  |
| ΣY   | 2.83  | 2.98  | 2.92  | 2.76  | 2.94  | 2.87  | 2.71  | 2.73  | 2.92  | 2.87  |
| X cations  |       |       |       |       |       |       |       |       |       |       |
| Ca <sup>2+</sup>   | 0.26  | 0.08  | 0.16  | 0.21  | 0.05  | 0.05  | 0.08  | 0.08  | 0.23  | 0.08  |
| Sr <sup>2+</sup>   | 0.01  | 0.01  | -     | 0.01  | -     | -     | 0.02  | -     | -     | -     |
| Na <sup>+</sup>  | 0.71  | 0.68  | 0.68  | 0.76  | 0.58  | 0.55  | 0.67  | 0.79  | 0.63  | 0.68  |
| K <sup>+</sup>   | 0.01  | -     | 0.01  | 0.01  | -     | -     | -     | -     | -     | -     |
| ΣX   | 0.99  | 0.77  | 0.85  | 0.99  | 0.63  | 0.60  | 0.77  | 0.87  | 0.86  | 0.76  |

932



933 **Table 4.** Major- and trace-element analyses of metarhyolite rock samples from Alpi  
934 Apuane studied in this work.

| Sample                             | <i>Fornovolasco Metarhyolite Fm</i> |       |       |       |       |        | <i>"Porfiroidi e scisti porfirici" Fm</i> |        |       |       |
|------------------------------------|-------------------------------------|-------|-------|-------|-------|--------|---|--------|-------|-------|
|                                    | FVb1                                | FVb2  | FVb13 | FVc2  | FVc8  | SAS1   | MUL1                                      | PORF1  | PORF2 | PORF3 |
| <i>Major elements (wt%)</i>        |                                     |       |       |       |       |        |   |        |       |       |
| SiO <sub>2</sub>                   | 73.18                               | 74.73 | 69.19 | 73.68 | 74.34 | 69.66  | 75.23                                     | 67.39  | 76.42 | 70.28 |
| TiO <sub>2</sub>                   | 0.24                                | 0.23  | 0.44  | 0.26  | 0.26  | 0.43   | 0.39                                      | 0.78   | 0.38  | 0.43  |
| Al <sub>2</sub> O <sub>3</sub>     | 13.60                               | 14.07 | 15.14 | 14.54 | 14.52 | 14.98  | 14.41                                     | 15.32  | 13.39 | 14.19 |
| Fe <sub>2</sub> O <sub>3 tot</sub> | 2.89                                | 1.74  | 3.30  | 1.80  | 2.02  | 2.94   | 1.20                                      | 5.52   | 1.60  | 3.24  |
| MnO                                | 0.01                                | 0.03  | 0.10  | 0.02  | 0.07  | 0.06   | 0.01                                      | 0.06   | 0.01  | 0.06  |
| MgO                                | 0.93                                | 0.72  | 1.46  | 1.31  | 0.67  | 1.71   | 0.50                                      | 1.47   | 0.69  | 0.65  |
| CaO                                | 0.17                                | 0.20  | 0.73  | 0.32  | 0.19  | 1.11   | 0.17                                      | 0.23   | 0.08  | 0.82  |
| Na <sub>2</sub> O                  | 0.29                                | 3.92  | 1.81  | 0.27  | 1.14  | 3.84   | 2.85                                      | 2.98   | 0.14  | 2.59  |
| K <sub>2</sub> O                   | 3.30                                | 2.38  | 4.54  | 4.57  | 3.74  | 2.68   | 3.03                                      | 3.38   | 4.42  | 4.95  |
| P <sub>2</sub> O <sub>5</sub>      | 0.13                                | 0.14  | 0.23  | 0.13  | 0.14  | 0.16   | 0.12                                      | 0.23   | 0.13  | 0.19  |
| LOI                                | 2.85                                | 1.45  | 2.33  | 2.49  | 1.75  | 2.48   | 1.86                                      | 2.64   | 2.18  | 2.18  |
| Total                              | 97.59                               | 99.61 | 99.27 | 99.39 | 98.84 | 100.05 | 99.77                                     | 100.00 | 99.44 | 99.58 |
| <i>Trace elements (ppm)</i>        |                                     |       |       |       |       |        |   |        |       |       |
| Be                                 | 4                                   | 3     | 4     | 4     | 4     | 3      | 2   | 3      | 3     | 2     |
| Sc                                 | 6                                   | 4     | 7     | 4     | 4     | 8      | 6   | 13     | 7     | 7     |
| V                                  | 23                                  | 21    | 47    | 28    | 27    | 49     | 43  | 74     | 26    | 34    |
| Cr                                 | < 20                                | < 20  | 50    | < 20  | 30    | 30     | 30  | 50     | < 20  | 30    |
| Co                                 | < 1                                 | 2     | 11    | < 1   | 4     | 5      | 2   | 12     | 1     | 8     |
| Ni                                 | < 20                                | < 20  | 30    | < 20  | < 20  | 20     | < 20                                      | 20     | < 20  | < 20  |
| Cu                                 | 260                                 | < 10  | 30    | < 10  | < 10  | < 10   | 40  | 20     | < 10  | 20    |
| Ga                                 | 17                                  | 14    | 17    | 18    | 18    | 16     | 15  | 20     | 17    | 18    |
| Ge                                 | 2.3                                 | 2.2   | 2.4   | 2.3   | 1.9   | 1.9    | 1.8                                       | 1.1    | 1.2   | 1.1   |
| As                                 | > 2000                              | 326   | 1120  | 75    | 58    | < 5    | 191                                       | 10     | 24    | 12    |
| Rb                                 | 116                                 | 99    | 214   | 176   | 124   | 86     | 110                                       | 112    | 138   | 111   |
| Sr                                 | 17                                  | 99    | 69    | 15    | 18    | 106    | 48  | 46     | 18    | 35    |
| Y                                  | 10.9                                | 8.4   | 18.2  | 12.3  | 11.5  | 16.6   | 16.4                                      | 40.9   | 36.6  | 35    |
| Zr                                 | 91                                  | 76    | 130   | 108   | 93    | 146    | 133                                       | 321    | 256   | 208   |
| Nb                                 | 7.1                                 | 7.0   | 7.5   | 8.0   | 7.1   | 7.8    | 6.1                                       | 14.9   | 11.1  | 11.6  |
| Ag                                 | 1.4                                 | < 0.5 | 0.6   | 0.6   | < 0.5 | 0.6    | 1.0                                       | 1.3    | 1.0   | 0.9   |
| Sn                                 | 24                                  | 10    | 10    | 17    | 17    | 3      | 5   | 3      | 3     | 4     |
| Sb                                 | > 200                               | 5.4   | 21.1  | 6.7   | 3.9   | 1.3    | 6.9                                       | 1.6    | 5.7   | 1.5   |
| Cs                                 | 5.7                                 | 8.6   | 21.9  | 5.8   | 3.9   | 3.3    | 6.1                                       | 5.1    | 8.4   | 6.0   |
| Ba                                 | 377                                 | 933   | 654   | 155   | 139   | 400    | 384                                       | 684    | 807   | 935   |
| Hf                                 | 2.4                                 | 2.1   | 3.3   | 2.8   | 2.6   | 3.7    | 3.5                                       | 8.1    | 6.1   | 5.4   |
| Ta                                 | 1.02                                | 1.46  | 0.98  | 1.14  | 1.13  | 1.03   | 0.94                                      | 1.03   | 0.92  | 0.95  |
| W                                  | 2.0                                 | 1.7   | 6.5   | 2.0   | 1.4   | 2.1    | 5.9                                       | 1.7    | 1.7   | 1.6   |
| Tl                                 | 2.68                                | 3.84  | 10.4  | 4.19  | 3.58  | 1.21   | 3.57                                      | 1.09   | 1.02  | 0.75  |
| Pb                                 | 1060                                | 48    | 256   | 22    | 13    | 6      | 157                                       | 21     | 27    | 12    |
| Bi                                 | 58.1                                | 3.3   | 50.8  | 38.9  | 1.6   | < 0.1  | 2.1                                       | 0.8    | 0.3   | 0.1   |
| Th                                 | 9.20                                | 5.52  | 9.58  | 10.1  | 9.36  | 10.2   | 9.19                                      | 19.3   | 18.3  | 15.9  |
| U                                  | 3.18                                | 2.69  | 4.44  | 1.82  | 1.72  | 2.05   | 2.11                                      | 3.03   | 2.94  | 4.13  |
| La                                 | 26.9                                | 16.5  | 24.5  | 37.7  | 24.7  | 21.1   | 26.1                                      | 55.5   | 62    | 47.1  |
| Ce                                 | 54.4                                | 34.8  | 50.8  | 76.5  | 48.2  | 42.3   | 49.0                                      | 118    | 125   | 95.4  |
| Pr                                 | 5.93                                | 3.91  | 5.70  | 8.51  | 5.56  | 4.9    | 5.98                                      | 13.3   | 13.9  | 10.9  |
| Nd                                 | 21.1                                | 14.0  | 20.6  | 31.0  | 20.6  | 17.9   | 22.5                                      | 50.4   | 51.1  | 40.7  |
| Sm                                 | 4.48                                | 2.97  | 4.56  | 6.47  | 4.34  | 3.97   | 4.58                                      | 10.4   | 9.78  | 8.50  |
| Eu                                 | 0.64                                | 0.692 | 0.966 | 0.949 | 0.621 | 1.04   | 0.741                                     | 1.38   | 1.23  | 1.23  |
| Gd                                 | 2.69                                | 2.28  | 3.93  | 4.48  | 3.05  | 3.48   | 3.79                                      | 9.01   | 7.84  | 7.55  |
| Tb                                 | 0.37                                | 0.33  | 0.56  | 0.57  | 0.43  | 0.55   | 0.60                                      | 1.35   | 1.11  | 1.18  |
| Dy                                 | 1.88                                | 1.73  | 3.12  | 2.58  | 2.12  | 3.12   | 3.25                                      | 7.58   | 6.30  | 6.64  |
| Ho                                 | 0.34                                | 0.30  | 0.56  | 0.41  | 0.37  | 0.58   | 0.6                                       | 1.44   | 1.2   | 1.23  |
| Er                                 | 0.99                                | 0.81  | 1.60  | 1.06  | 1.05  | 1.55   | 1.75                                      | 4.03   | 3.45  | 3.39  |
| Tm                                 | 0.155                               | 0.119 | 0.214 | 0.134 | 0.147 | 0.227  | 0.235                                     | 0.585  | 0.504 | 0.455 |
| Yb                                 | 1.04                                | 0.77  | 1.38  | 0.83  | 0.99  | 1.60   | 1.57                                      | 3.89   | 3.32  | 2.93  |
| Lu                                 | 0.166                               | 0.123 | 0.228 | 0.131 | 0.152 | 0.234  | 0.248                                     | 0.560  | 0.496 | 0.475 |

935  
936

937 **Table 5.** Summary of LA-ICP-MS U-Pb zircon datings of the Fornovolasco metarhyolite.

| Sample | Zircon crystals<br>imaged by<br>SEM-CL | Zircon crystals<br>selected for U-Pb<br>dating | LA<br>spots | Number of U-<br>Pb concordant<br>ages* |     | Age (Ma)                  |              |              |
|--------|--|--|-------------|--|-----|---------------------------|--------------|--------------|
|        |  |  |             |  |     | weighted<br>average (±2σ) | min (±2σ)    | max (±2σ)    |
| FVb13  | 116                                    | 82   | 122         | rims                                   | 36  | 271.0 (±3.5)              | 241.8 (±4.0) | 300.8 (±4.7) |
|        |  |  |             | cores                                  | 10  | 276.8 (±8.8)              | 260.3 (±7.2) | 298.1 (±4.5) |
| FVc1   | 80                                     | 61   | 85          | rims                                   | 40  | 279.7 (±3.4)              | 256.0 (±6.2) | 296.4 (±3.5) |
|        |  |  |             | cores                                  | 7   | 282.6 (±6.6)              | 270.0 (±5.6) | 293.7 (±5.5) |
| POL1   | 107                                    | 55   | 73          | rims                                   | 24  | 276.7 (±8.5)              | 226.5 (±6.3) | 306.1 (±6.3) |
|        |  |  |             | cores                                  | 0   | -                         | -            | -            |
| SAS1   | 114                                    | 80   | 106         | rims                                   | 44  | 291.8 (±3.2)              | 258.6 (±6.6) | 310.6 (±5.4) |
|        |  |  |             | cores                                  | 8   | 290.2 (±6.2)              | 280.7 (±4.8) | 300.9 (±5.4) |
|        |  |  |             | All                                    | 169 | 279.9 (±2.0)              |              |              |

\*The cutoff limit was set to 3% normal discordance  $\{[(^{206}\text{Pb}/^{238}\text{U age})/(^{207}\text{Pb}/^{235}\text{U age}) - 1]*100\}$ .

938  
939

Figure 1  
[Click here to download high resolution image](#)

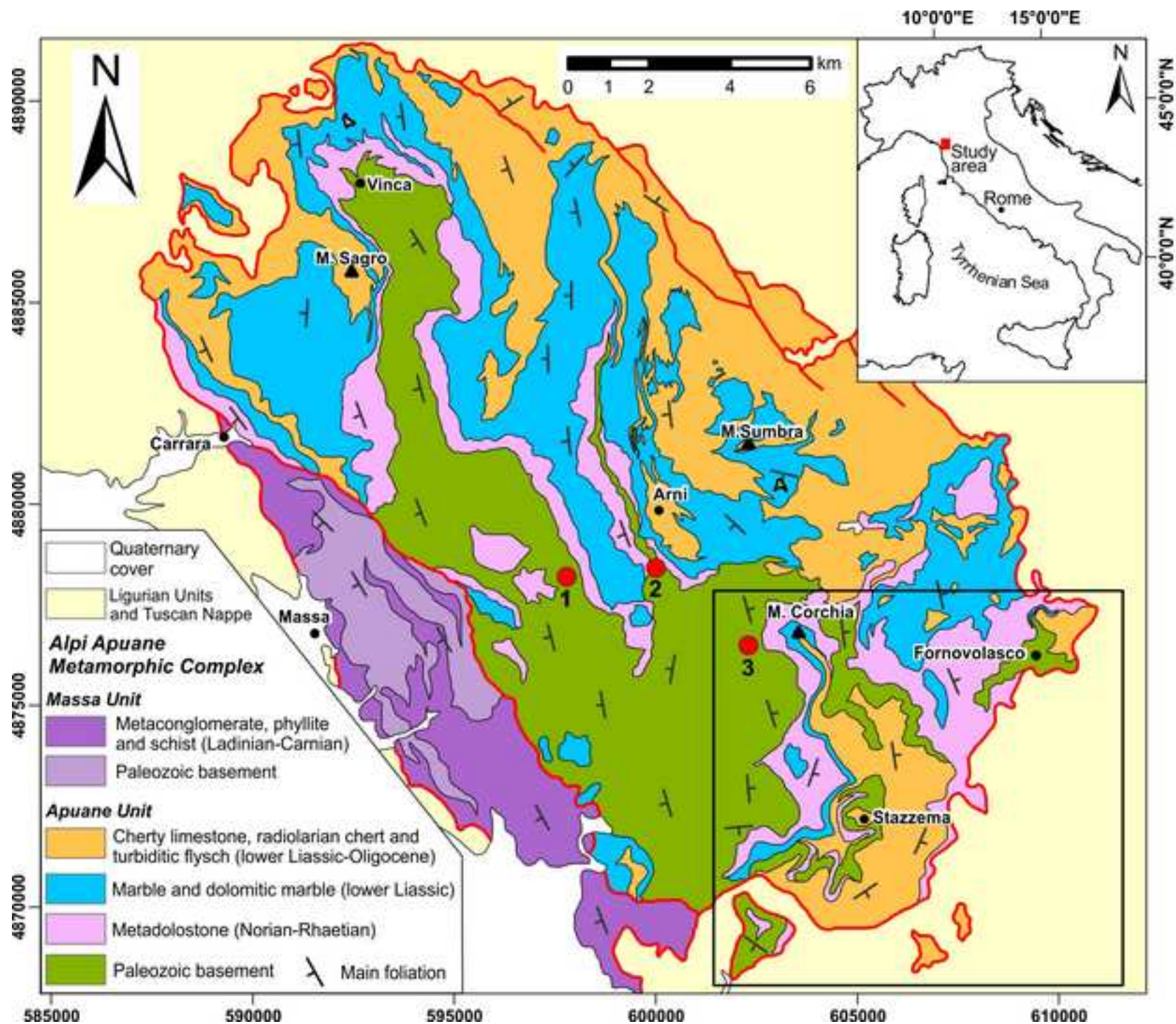




Figure 2  
[Click here to download high resolution image](#)

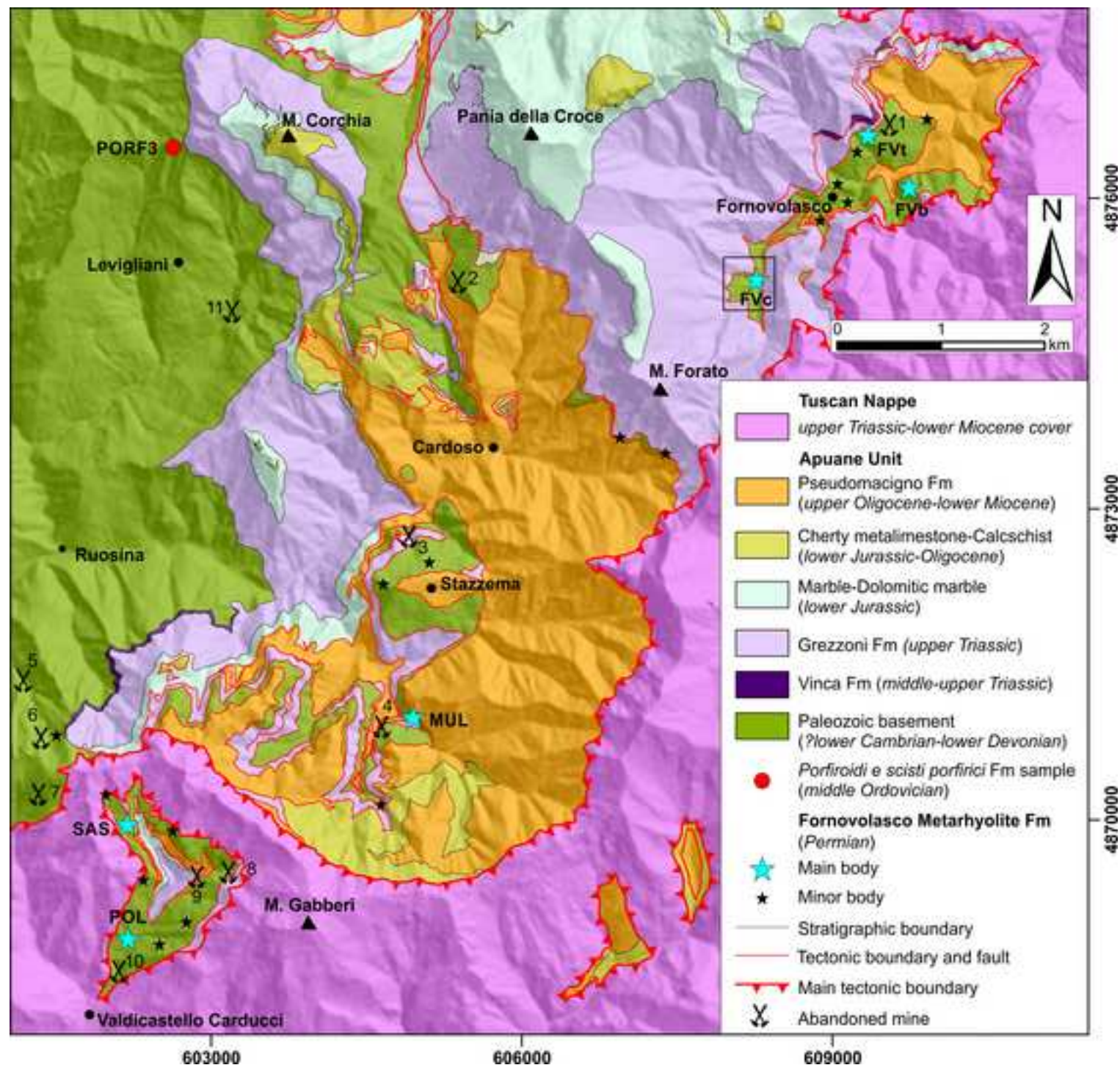




Figure 3  
[Click here to download high resolution image](#)

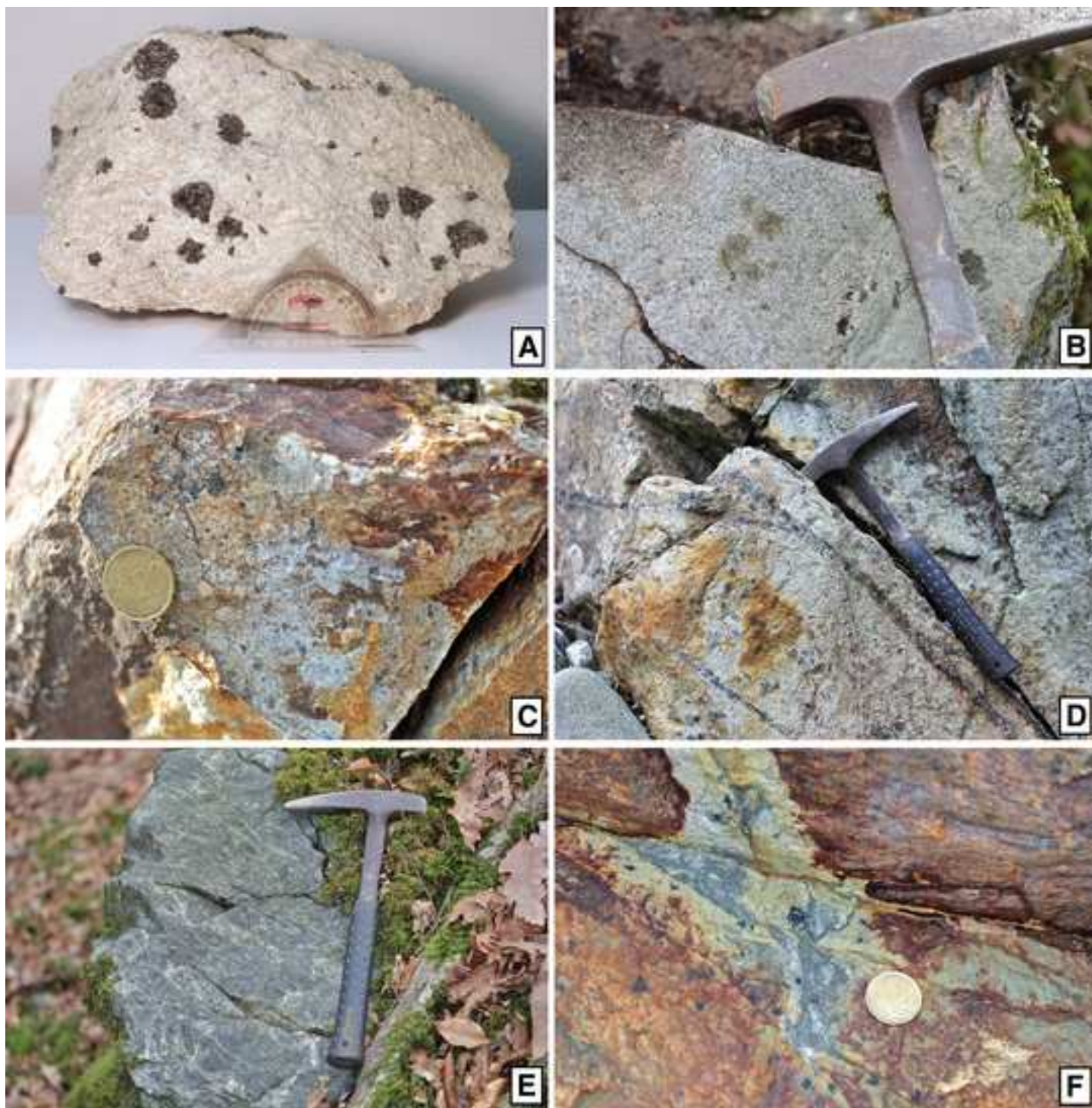




Figure 4  
[Click here to download high resolution image](#)

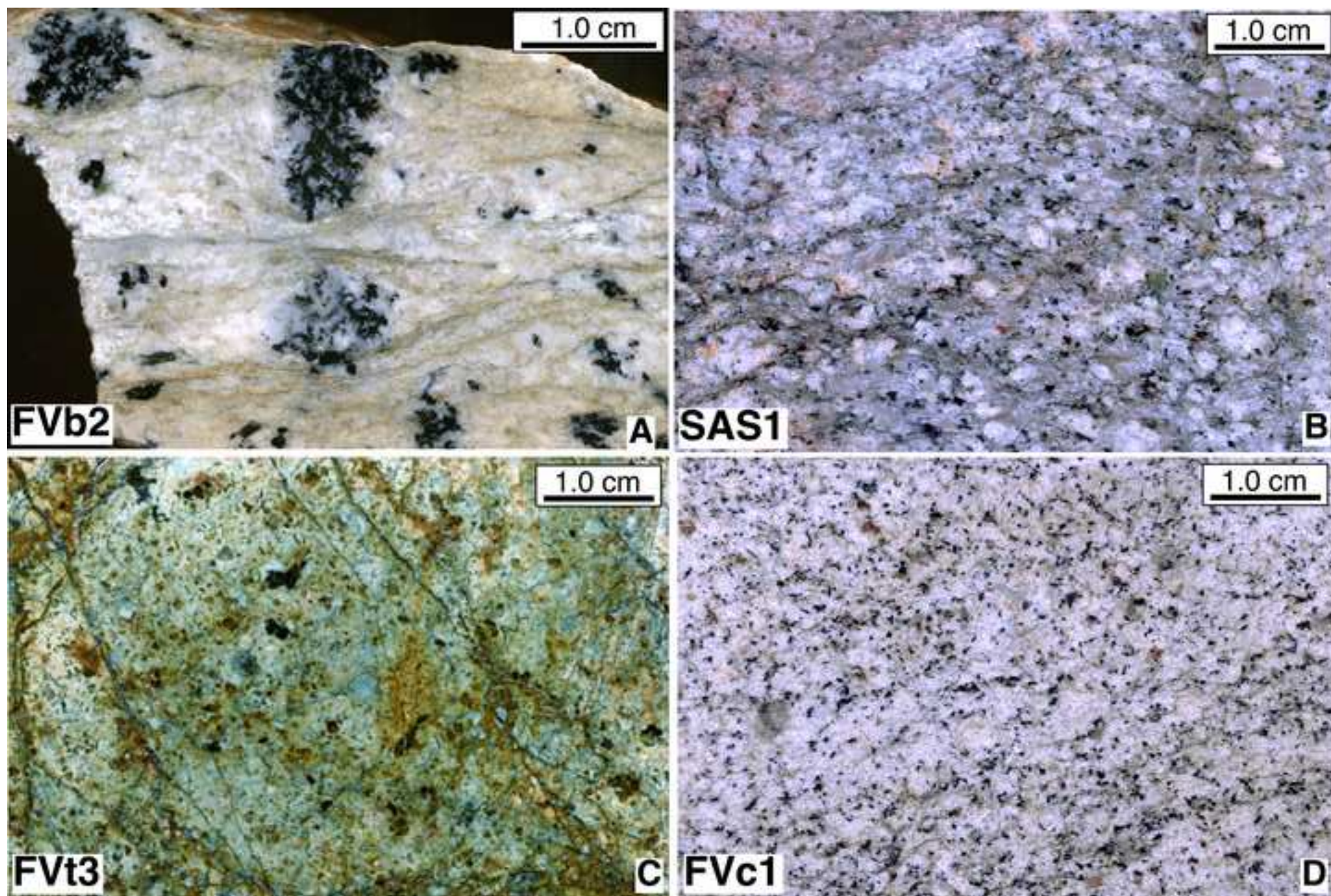




Figure 5  
[Click here to download high resolution image](#)

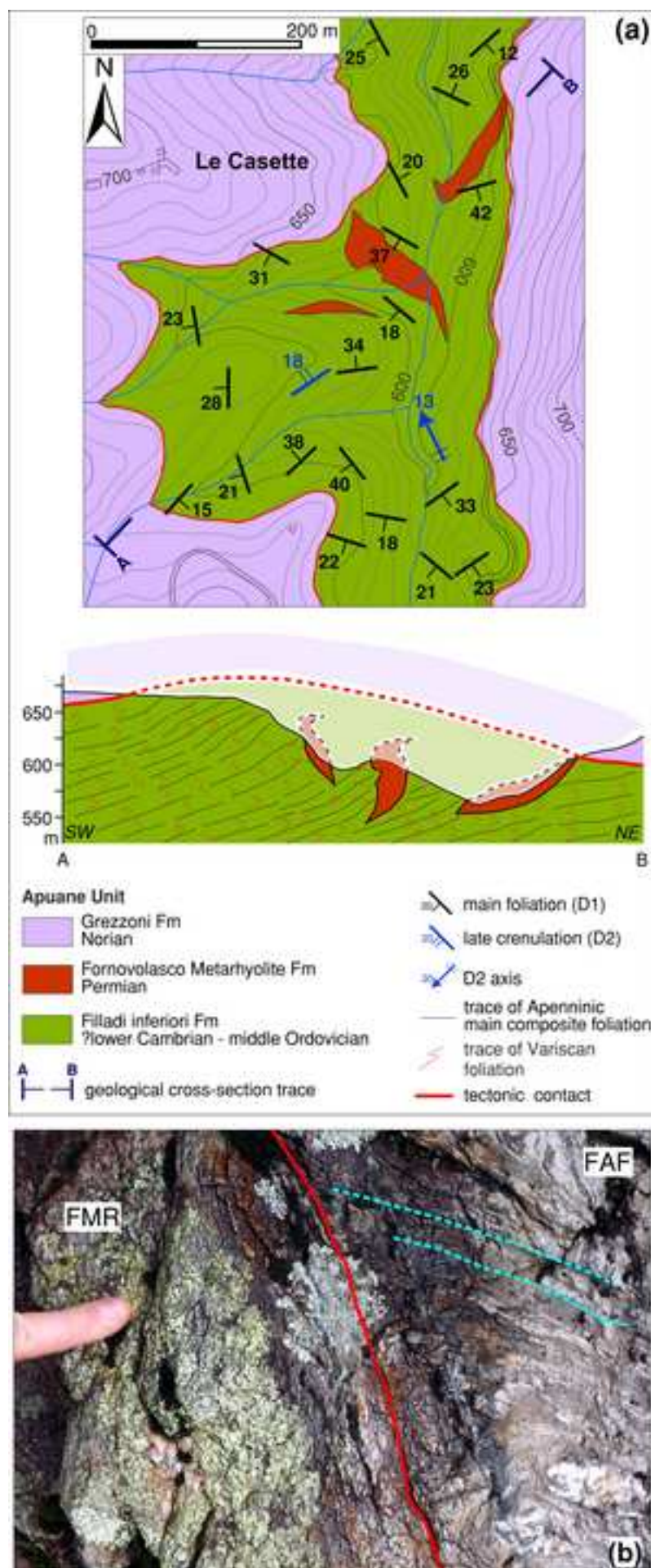




Figure 6  
[Click here to download high resolution image](#)

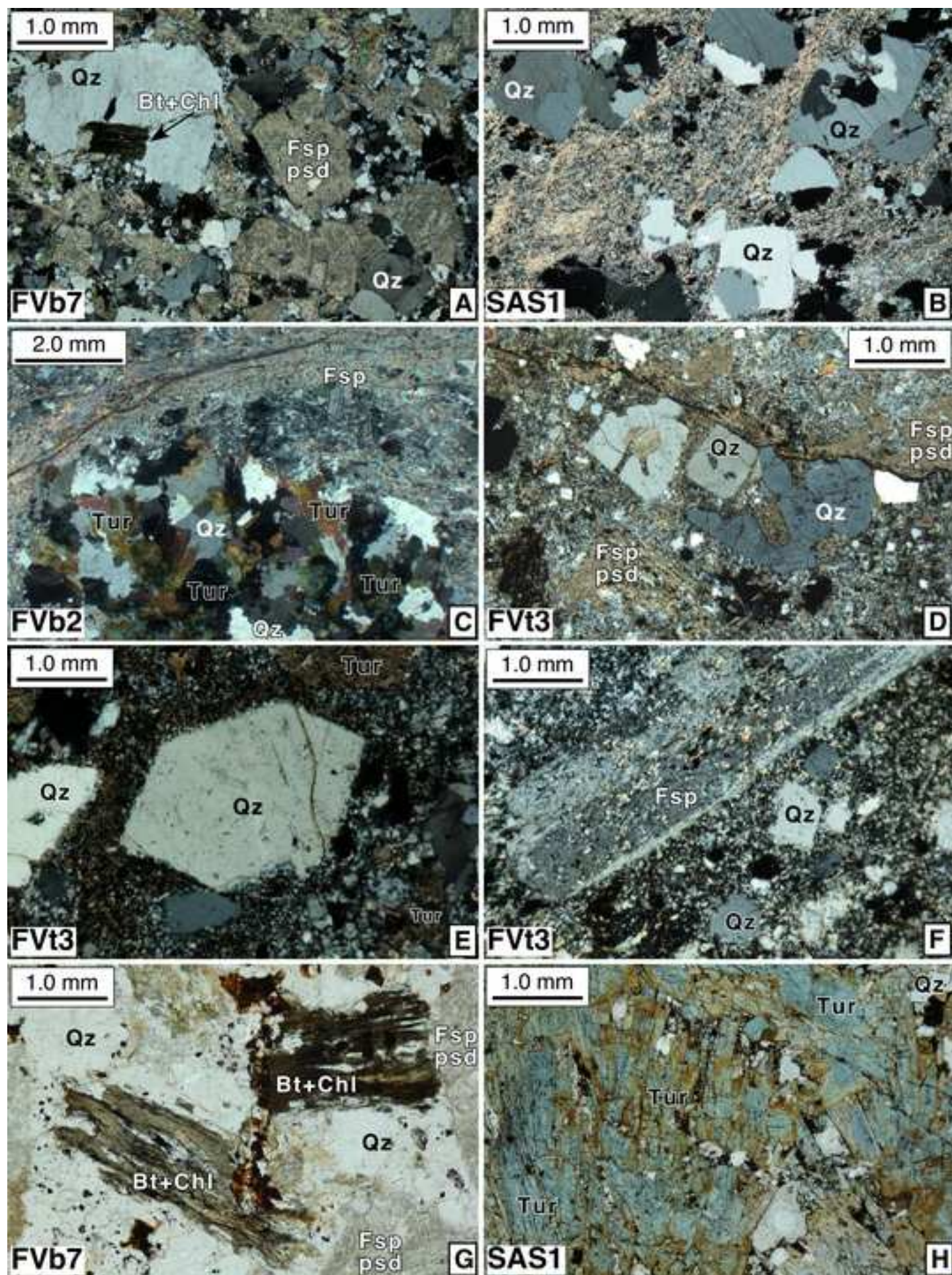




Figure 7  
[Click here to download high resolution image](#)

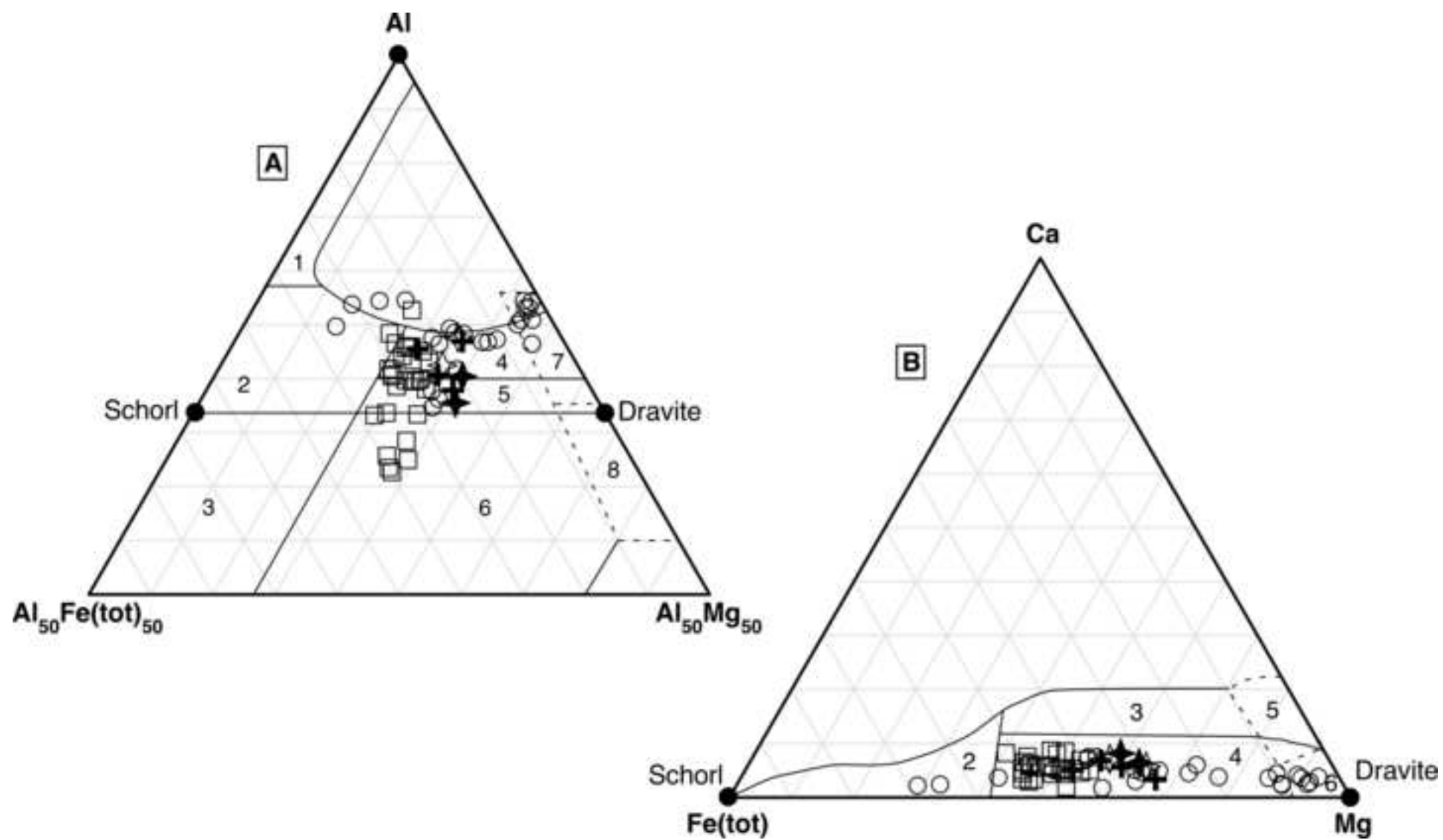


Figure 8  
[Click here to download high resolution image](#)

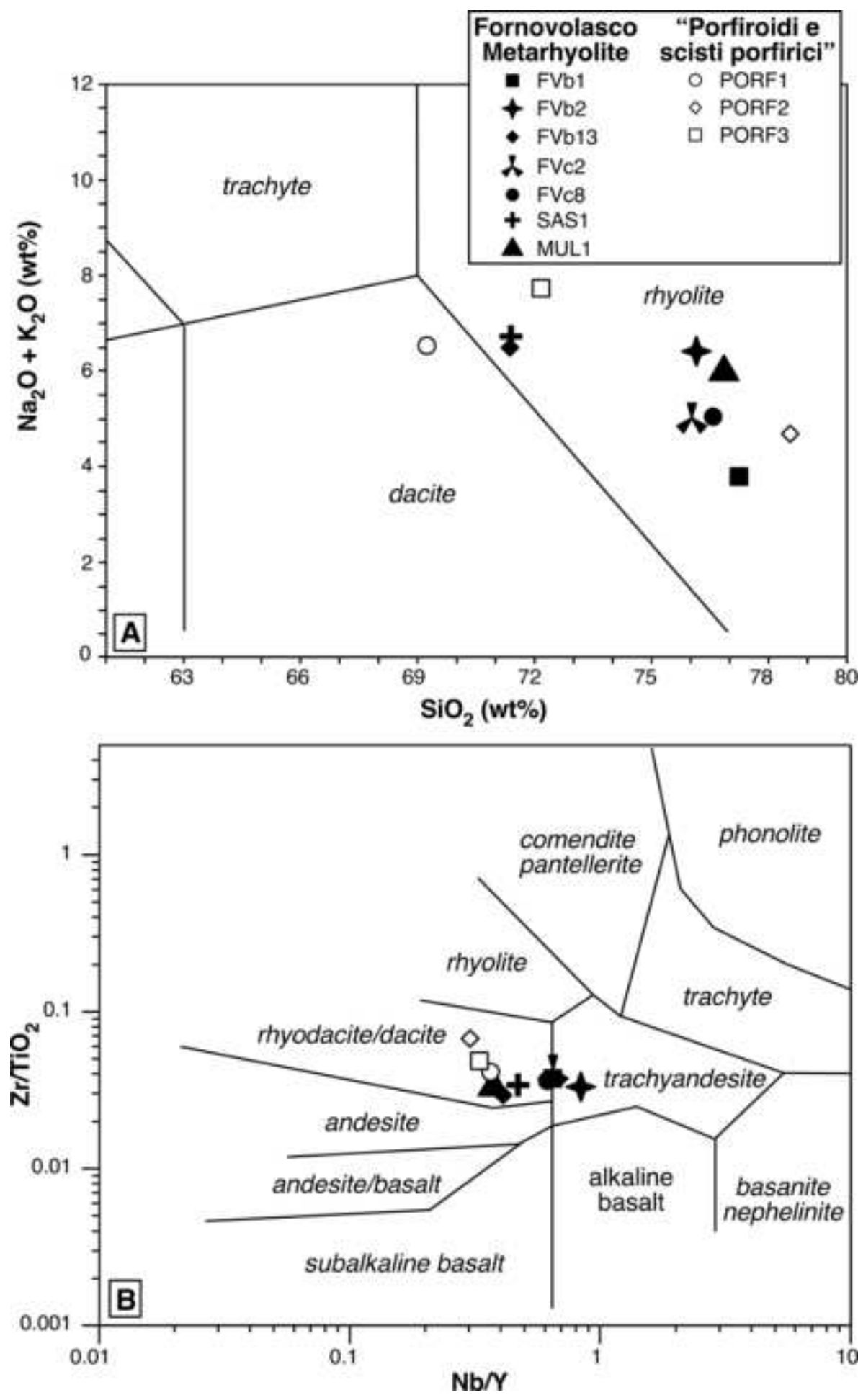


Figure 9  
[Click here to download high resolution image](#)

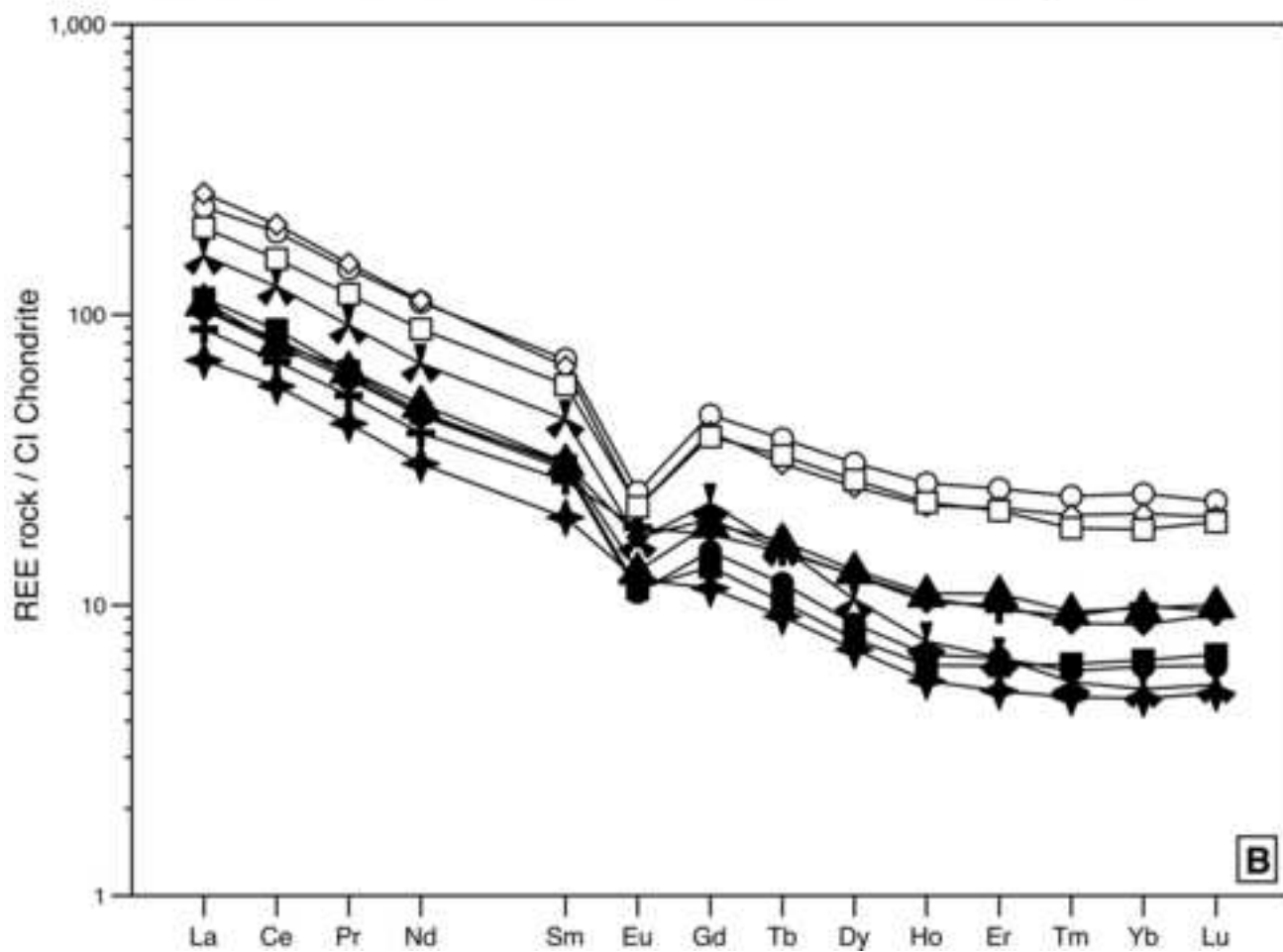
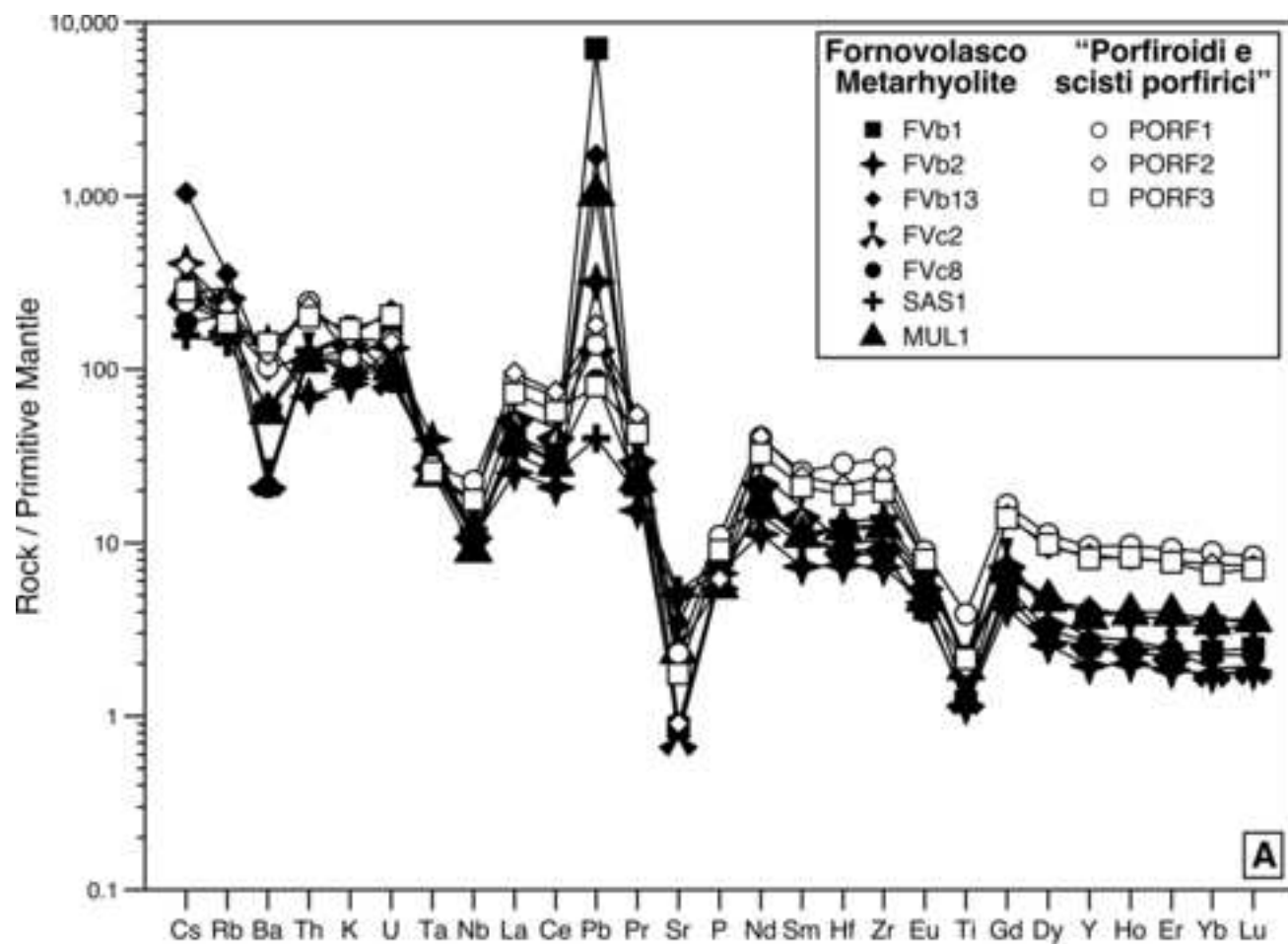


Figure 10

[Click here to download high resolution image](#)

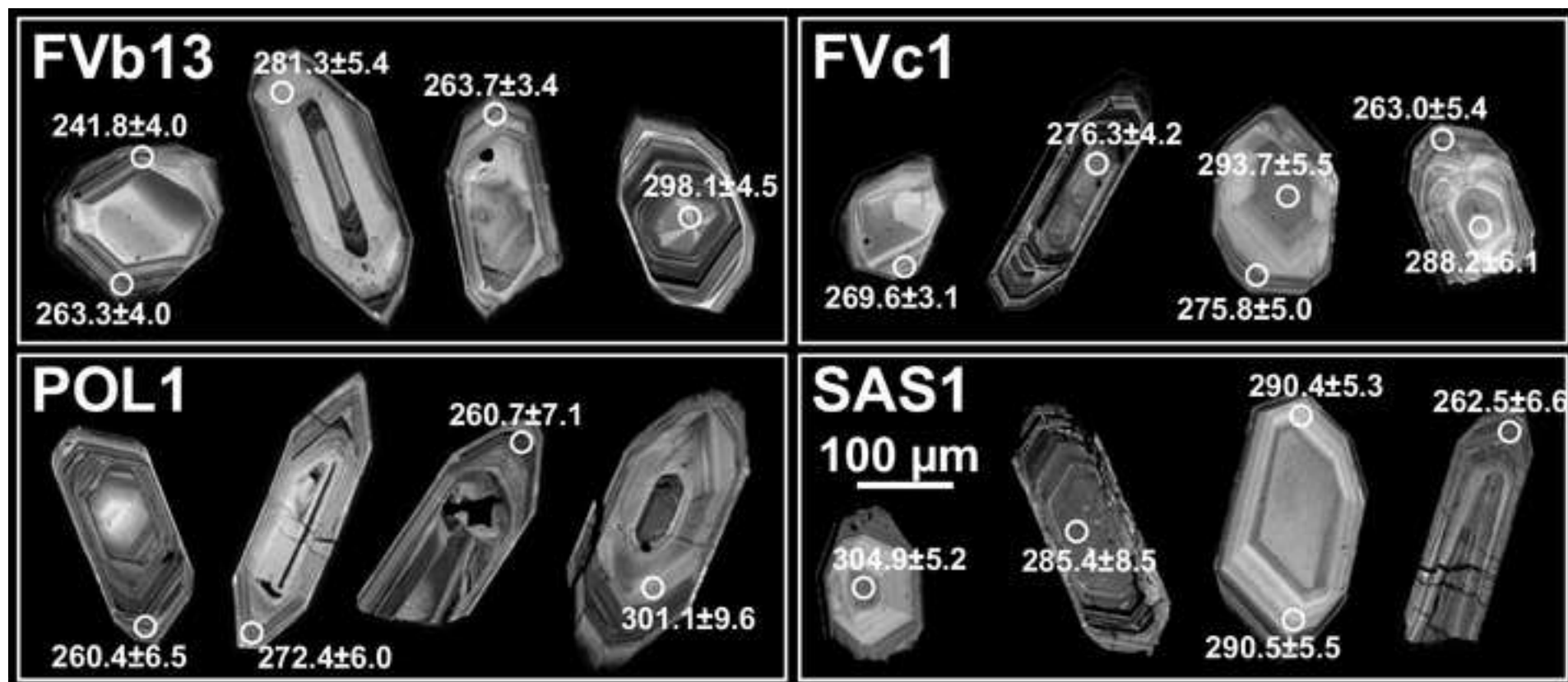


Figure 11  
[Click here to download high resolution image](#)

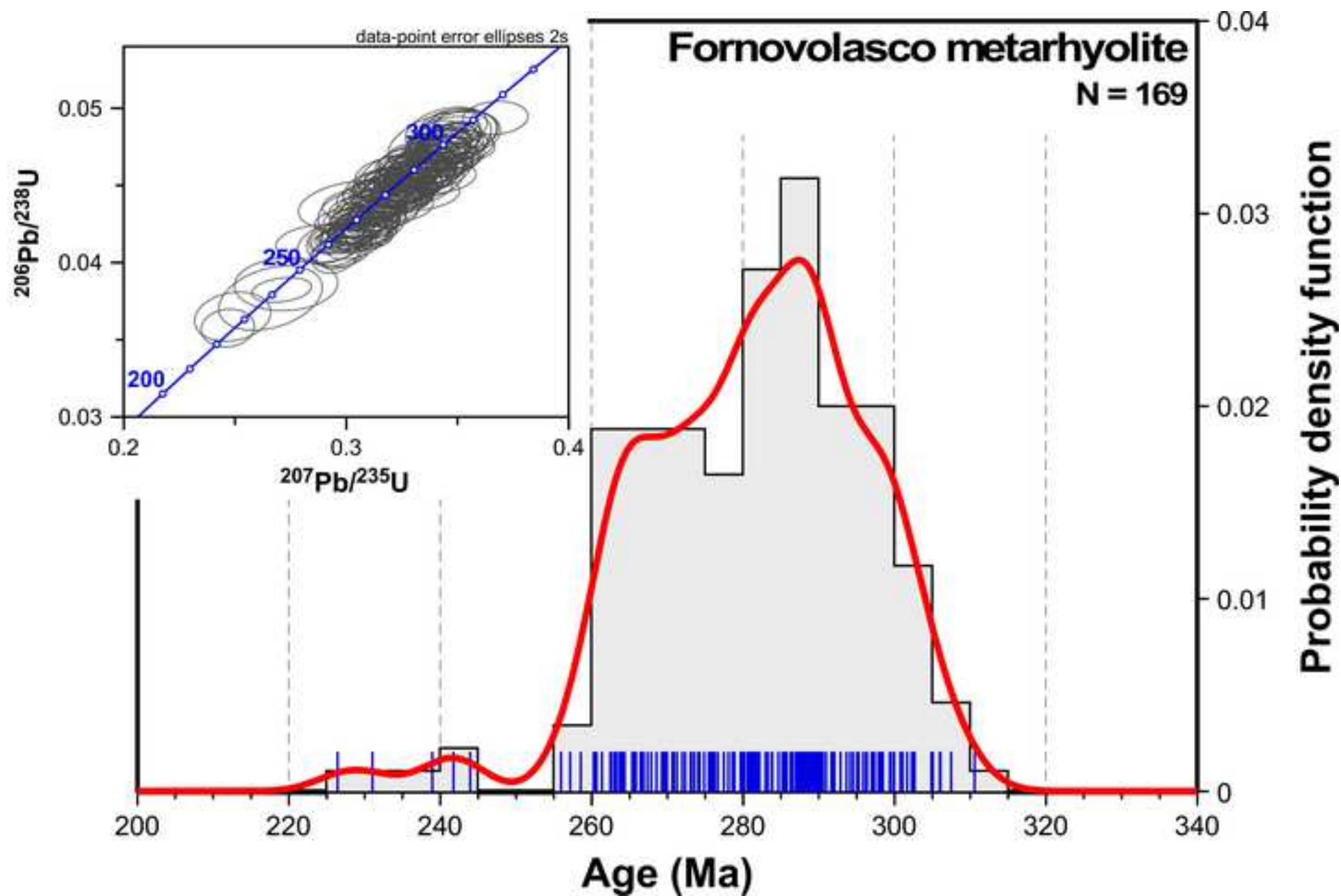




Figure 12  
[Click here to download high resolution image](#)

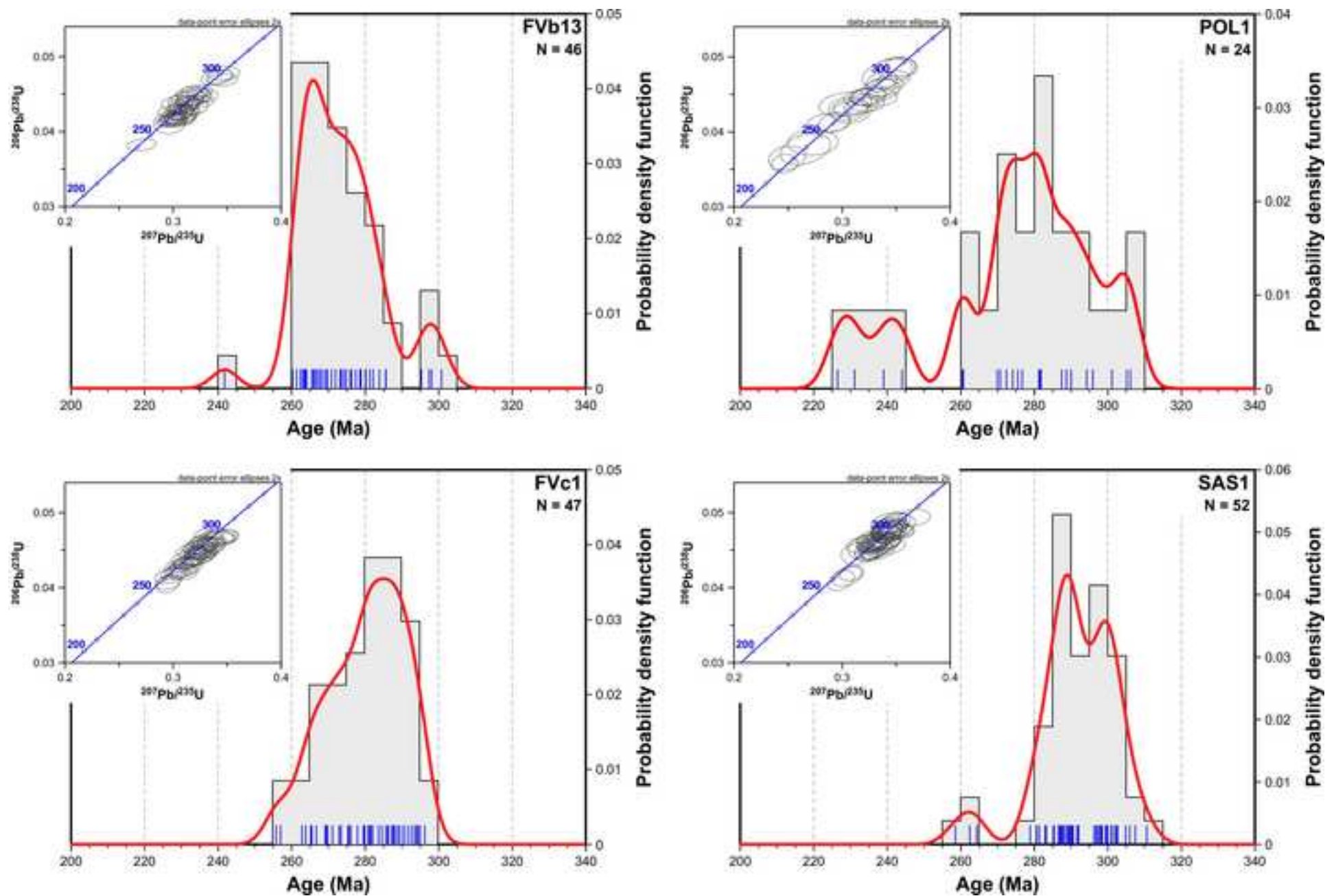


Figure 13

[Click here to download high resolution image](#)

